Psychological Review

Allometric Scaling Laws for Temporal Proximity in Perceptual Organization

David L. Gilden and Taylor M. Mezaraups

Online First Publication, July 1, 2021. http://dx.doi.org/10.1037/rev0000307

American Psychological Association

Psychological Review

ISSN: 0033-295X

https://doi.org/10.1037/rev0000307

Allometric Scaling Laws for Temporal Proximity in Perceptual Organization

David L. Gilden and Taylor M. Mezaraups
Department of Psychology, University of Texas at Austin

In both space and time, proximity plays an important role in the formation of perceived groups, objects, and scenes. Proximity is especially critical in the temporal domain where there are constraints—pauses or delays between neighboring events, that when of sufficient size, defeat the grouping processes that underlay temporal integration. A framework is developed where temporal proximity constraints are theorized to reflect lifetimes of exponential decay processes, and this identification leads to an inquiry into their scaling properties. In a study focusing on rhythmic pulse, the slowest tempo permitting stable rhythmic performance is shown to satisfy an allometry with a power-law exponent close to that of heart rate. The coefficient of variation, a measure of drumming stability and precision, is also shown to obey an allometry. A theory is developed that predicts that allometry in the coefficient of variation exists only at adagio and largo tempi. In a second experiment, this theory is tested by replicating the finding of precision allometry at 60 bpm, and by finding that precision is independent of body size at the marching tempo of 120 bpm. A third experiment examined proximity constraints in apparent motion, historically a defining example of temporal organization. Using a behavioral method for measuring path vividness, it is demonstrated that proximity constraints for the percept of illusory motion paths also satisfy an allometry. These two examples of proximity constraint scaling suggest that allometry may be a generic feature of temporal integration.

Keywords: allometry, gestalt, perceptual organization, rhythm, apparent motion

There are at least two distinct points of departure for studying timing in animals. One is principally concerned with explicit judgment and begins with the observation that people and other animals are able to judge the magnitudes of time intervals. Many of the same issues that animated much of early sensory psychophysics have been recapitulated in the arena of time judgment (Allan, 1979; Fraisse, 1984; Grondin, 2010; Wearden, 1991). The second point of departure concerns the implicit appearance of time in the organization of perception and action. Beyond issues of what people know about time and time intervals is the patent observation that the temporal flux of ordinary experience is perceptually organized, integrated, into distinct, and segmented scenes. Scene formation is what transforms the flow of time into a coherent and meaningful world.

In the context of judgment, time intervals are treated as objects that may be attended to and which have properties such as their magnitude and whether they are filled or unfilled. In psychophysical assessments of judgment, these objects are presented as stimuli in an experimental design that is divorced from the contexts in which time enters an animal's life as temporality. Of particular relevance to the work presented here is the circumstance that the specific time interval magnitudes that appear in the experimental design are freely chosen to address the hypotheses being tested. Consequently, it is not uncommon for people and other animals (rats and pigeons in particular) to be placed in situations where they are asked to judge time intervals that are quite large, extending to several scores of seconds (Roberts, 1998). Typical studies in these interval regimes (see for example Catania, 1970; Roberts, 1981; Roberts & Church, 1978) have revealed that time interval judgment has much in common with magnitude estimation generally; errors are typically Weberian (errors scale with the size of the thing being judged), and representations appear to be compressive.

In the context of perceptual organization, time is not an object of judgment but a background dimension in the physical sense where events are marked by the moments of their occurrence. These moments are graded by proximity, a construct that is a relational property of events and which is distinguished from magnitude which is a property of time intervals. Proximity is generally a key determinant of grouping, and there are many points of commonality between how it functions in space and how it functions in time. Nevertheless, temporal proximity has key structural differences from spatial proximity.

In spatial organization, proximity is relative in that the influence it has over grouping may be invariant over transformations in overall scale. A given picture, for example, can be magnified or shrunk without changing any characteristic of grouping or shape. The implication is that spatial proximity is not graded in terms of meters or degrees of arc but more abstractly in terms of the entire set of distance relations that exist in any given scene. Furthermore, there is no spatial displacement that sets an absolute limit on whether

David L. Gilden https://orcid.org/0000-0002-5820-3076
Taylor M. Mezaraups https://orcid.org/0000-0002-9380-4635

David L. Gilden developed the study concept and study design. Testing and data collection were the primary responsibility of Taylor M. Mezaraups. Both authors conducted the data analyses. David L. Gilden drafted the article with editorial advice from Taylor M. Mezaraups. Both authors approved the final version of the article. The authors thank Lydia M. Crooks for her assistance in collecting and analyzing data and Jesse L. Martz for helping in the collection of data. The ideas and data presented in this article have not been disseminated prior to publication.

Correspondence concerning this article should be addressed to David L. Gilden, Department of Psychology, University of Texas at Austin, 108 E. Dean Keeton Stop A8000, Austin, Texas 78712, United States. Email: dgilden@utexas.edu

elements in a scene will be grouped. When grouping is not decided solely on the basis of proximity, it is because there is some other principle (similarity, continuity, closure, etc.) that happens to be more effective in that particular arrangement. In this sense, spatial grouping principles are not binary in their effectiveness, but rather their effectiveness is continuously graded in the sense of a competition (Quinlan & Wilton, 1998). The fact that spatial proximity is invariant under transformations of scale, and is always competitive in grouping, means that there is no such thing as a proximity constraint in spatial organization. It is on this point that temporal proximity and spatial proximity diverge because there are temporal proximity constraints.

Temporal organization has the interesting feature that there are upper bounds on the lengths of delays or pauses that may be tolerated in the formation of groups and scenes. That some upper bound exists for the integrative processes that effect temporal scene formation may not be surprising, but it is significant that upper bounds are often found to have values in the range of 2 ± 1 s. Although the conduct of ordinary life is literally composed by the processes of temporal integration, a few explicit examples may serve to illustrate the many ways that the emergent properties associated with temporal organization dissolve into temporal succession when gaps of just a couple of seconds are interposed. These few examples are intended to simply make the point that proximity constraints of 2 ± 1 s are a common feature of perceptual organization in time. Whether or not 2 ± 1 s reflects the span of the subjective present (Pöppel, 1997, 2009), or whether it is relevant to all forms of temporal integration (White, 2017), is not at issue here.

Musical Experience

The abilities of people to produce and comprehend music is limited to specific regimes of tempo. The experience of rhythmic pulse, in particular, is severely attenuated at tempi much slower than 40 bpm. A percussionist, say, playing a duple rhythm at tempi greater than 40 bpm will experience successive beats[1] in relation to one another, and the performance will generate a sense of rhythmic pulse. The same duple rhythm played slower than about 40 bpm leads to a very different experience. When moments of beat production are separated by more than about 1.5 s, successive beats lose their sense of being connected and are experienced rather as a succession of individual and discrete moments. The aspect of perceptual organization known as melody also mostly disappears when note onsets are separated by more than about 1.5 s (Warren et al., 1991). When common melodies are given note durations of about 1.5 s, they become unrecognizable, evidently sounding more like note successions than songs.

Apparent Motion

The most well-studied example of temporal integration in cognitive psychology is long-range apparent motion. β movement, originally investigated by Wertheimer (1912), is a paradigmatic example of an emergent quality (Steinman et al., 2000) that fails to appear when a proximity constraint is violated. Under optimal timing parameters, two alternating images will appear to fuse into one as an illusory path emerges. However, when the stimulus onset asynchrony (SOA) approaches 700 or 800 ms, the single fused object will dissolve, and the (veridical) succession of two blinking images (Ekroll et al., 2008) will be recovered.

Segmentation

The observation that pauses generally act as temporal scissors to segment and separate the stream of happenings is so fundamental to ordinary experience that it is unnecessary to reference psychophysics. For the purposes of illustration and to get a sense of what a pause of a couple seconds can achieve, it is instructive to review how pauses are used informally in the methods sections of the psychological literature—where experimental psychologists reveal their implicit understandings of temporality. As an example, consider how lists are presented in, say, a word learning experiment. In this context, pauses are inserted so that the list is not heard as an intact sentence but as a succession of separate items. Roediger and McDermott (1995), to take an often-cited article, use 1.5 s to separate words. This choice does not reflect a psychophysical measurement of the transition for words heard in phrases to words heard as isolated items; the choice simply reflects their experience, as listeners, with pause lengths that can effectively create segmentation without wasting time. Of note, 1.5 s suffices for the purpose of list presentation. Similarly, if an experimenter wishes to give participants a clear sense of beginnings and endings of trials beyond the sense of ending that is provided by response, a second or two waiting time is imposed. Again, to reference an often-cited article, Meyer and Schvaneveldt (1971) employ an intertrial interval of 2 s. This interval is, again, not derived from psychophysics but reflects the investigator's implicit understanding of what is required for a participant to receive feedback and get themselves ready for the next scene, or in this case, the next trial. Longer intertrial intervals could have been employed, but ordinary experience provides innumerable tutorials in event segmentation; the choice of 2 s is far from arbitrary. In this way, the psychological literature methods sections may be viewed as an informed distillation of how much time is required to cognitively dissociate a stimulus stream into discrete trial events. And, it is worth emphasizing that such choices are neither justified nor called into question, implying that this aspect of temporality is held in common.

Causal Learning

The delay of reinforcement gradient is the most well-studied example of proximity constraint in the formation of an emergent grouping. It captures how a delay between two events, an operant and a reinforcer, influences the learning of a causal relation—the sense that not only were there two events, one following the other, but also that one *caused* the other. Much of the early work on the delay of reinforcement gradient can be summarized by the finding that a delay of just a few seconds suffices to severely attenuate the causal association of, say, a bar press and the appearance of a food pellet (Perin, 1943). The critical role that a few seconds plays in determining whether events are perceived in terms of actions and

[1] Although it is common in psychological contexts to regard beat as being synonymous with pulse, beat here is used within common musical terminology to denote a distal event or musical structure independent of how that event or structure is experienced. So a time signature is defined by the number of beats per measure, and beat machines generate pulse through the production of dance beats, rap beats, pop beats, and so forth.

consequences, a type of grouping, is well known to anybody who has attempted to train an animal to enact specific behaviors.

The experimental work presented in this article grew out of an attempt to understand the mechanisms of temporal organization that lead to every grouping process having a proximity constraint, and further, to understand why these constraints appear to have fairly restricted values. This inquiry led to the conjecture that proximity constraints might not have fixed values but rather function as timescales that have parametric dependencies. As timescales in living systems are often parameterized by body size, our investigations focus on determining whether proximity constraints satisfy allometric laws, and if so, what interpretation may be brought to the derived exponents. We begin with a brief review of the theoretical issues.

Theory of Temporal Proximity Constraints

In this section, we consider what mechanisms might produce temporal proximity constraints. As a vehicle for this discussion, we will focus on the phenomenon of rhythmic pulse, as it is universally familiar, and there are widely divergent accounts for why pulse fails at tempi much slower than 40 bpm. An influential theory of pulse and one that provides a strong contrast with a perceptual integration perspective is entrainment theory (Large, 2000; Large & Kolen, 1994; Large & Palmer, 2002; Large & Snyder, 2009; Thut et al., 2011). In entrainment theory, the experience of pulse and meter arises from the coupling of neural oscillations in the brain with periodic signals in the environment. Essentially, the brain uses its resonant structures to manifest patterns that are coordinate in the environment (Large & Jones, 1999). In this view, the reason people are unable to experience rhythmic pulse at very slow tempi, say slower than 30 or 40 bpm, is that there are no sustained brain oscillations at frequencies below ½ Hz that are available to entrain to a ½ Hz environmental signal (Bååth, 2015). Large and Kolen (1994) refer to this circumstance as the environmental signal falling outside of the receptive fields of available neural oscillations. To this extent, pulse constraints at slow tempi might be viewed as similar in kind to constraints on spatial frequency processing in vision; structures in light that have spatial frequencies below about 0.1 cycles/deg are essentially invisible. The low-frequency cutoff for contrast sensitivity function is not viewed as a failure of perceptual organization, and neither is the loss of rhythmic pulse at slow tempi in entrainment theory.

An account of rhythmic experience from the point of view of perceptual organization views pulse as an emergent property of individual beats being perceived in relationship with neighboring beats. In this view, pulse arises from group formation, and when pulse fails to be experienced, it is because there are temporal limitations on the processes that allow neighboring beats to be relatable. Mates et al. (1994) theorize that such limitations are consequent to activation decay within an implicit working memory system. Specifically, they theorize that the experience of a beat creates a short-term memory trace that "fades out" over 2 to 3 s, after which it can no longer serve as a reliable cue for the placement of a subsequent beat.

These two accounts of how pulse acquires a proximity constraint are distinguished by their potential for generalization. In entrainment theory, pulse will fail to be produced when the brain does not supply oscillations at a frequency that might couple to a slowly varying environmental signal. In this sense, failure occurs for reasons that are intrinsic to pulse mechanics and would not generalize to other forms of temporal grouping.[2] The perceptual organization account, in contrast, acquires considerable generality by placing the origin of proximity constraints in a memory system that is structurally separate from the mechanisms that effect the formation of temporal groups. To the extent that temporal integration generally involves a form of implicit memory, activation decay provides a mechanism for creating proximity constraints in all forms of temporal grouping.

A general theory of proximity constraints comes to down to three principles: That event onsets create activation, that grouping processes act on activation overlap between neighboring event onsets, and that activation decays. What counts as an event here is intentionally left unspecific. An event could be a beat, a note, a word, an image, a head nod—anything that might be brought into a temporal relationship to create a group. Figure 1 shows the theory and how decay and overlap are the decisive constructs that create a proximity metric that sets what is near and far in time. In this picture, proximity constraints are experienced when the temporal gap between neighboring events exceeds the activation lifetime. The observation that many proximity constraints converge on a common value, 2 ± 1 s, is interpreted as a consequence of various grouping mechanisms sharing a common scheme of activation.

Theory of Decay

The experimental work presented in this article was motivated by considering whether the functional form of activation decay might be described by a negative exponential,

$$X(t) = X(0) * e^{-t/\tau},$$

where τ is the activation lifetime, or more formally, the e-folding time. Decay processes are often observed to be negative exponentials simply because the underlying differential equation describes a situation often encountered in natural systems; the loss rate is proportional to the amount that is present to lose:

$$dX/dt = -kX \quad (1)$$

where $k = 1/\tau$ is a constant. This differential equation is also the simplest nontrivial description of a decay process; it is linear in the decaying quantity and there is no explicit time dependence. Finally, Equation 1 may be viewed as a universal decay equation for small perturbations. Any decay process $dX/dt = -F(X)$ where F is a positive definite function will yield Equation 1 in a Taylor expansion of F to first order.

The issue of explicit time dependence in decay rate is important in evaluating whether the negative exponential applies in a given situation. In the context of long-term memory, for example, Simon (1966) considered the negative exponential as a candidate expression for forgetting but rejected it in view of Jost's second law—the observation that older memories decay more slowly than younger

[2] In fairness, entrainment theory and other schemes for extracting pulse from periodic beat trains (Scheirer, 1998; Eck, 2006) are not designed to explain pulse proximity constraints. Rather, they are intended to provide formal theories of the basic phenomenon that pulse is experienced in the presence of a periodic signal.

Figure 1
A Sketch of the Framework Where Proximity Constraints Are Set by Activation Lifetimes

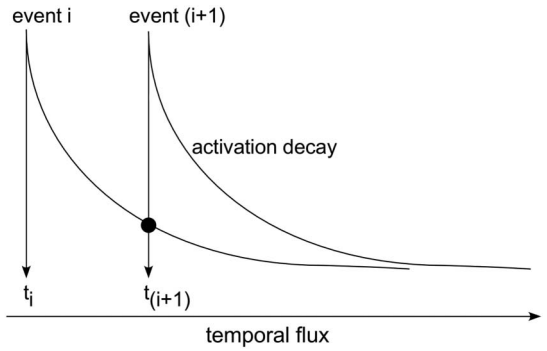

Note. Neighboring events in time are available for integration into groups to the extent that later events arrive before the activation produced by earlier events has decayed.

memories. A rate equation that is consistent with Jost's second law may be constructed by simply introducing a factor of 1/t into Equation 1. With this modification, the decay rate given in Equation 2 is an explicit function of memory age such that, given two memories of equal strength, the older one will decay more slowly.

$$dX/dt = -kX/t. \tag{2}$$

The explicit time dependence in Equation 2 leads to the familiar power law of forgetting,

$$X(t) = X(0)(t_0/t)^k,$$

and while it is difficult in practice to distinguish power laws from exponentials in data (Navarro et al., 2004), the two laws are distinguished by having different metrics for the time passage. The exponential decay law has a timescale, τ, that provides an intrinsic ruler for time passage: For every additional interval of elapsed time equal to τ, activation decreases by a factor of e. Time is not scaled in this sense in a power law; time is measured just as clock time since the onset of forgetting. The question of whether activation decay is measured by a timescale comes down in part to deciding whether the decay rate is time independent.

To evaluate whether the exponential is a viable model for activation decay, we consider what processes in long-term memory cause the loss rate to acquire time dependence and whether such processes might play a role in the brief activation decay that is relevant to the formation of proximity constraints. Wixted (2004), in a thorough review of Jost's second law, concludes that time-dependent decay rates occur in long-term memory as consequence of processes of consolidation that render older memories less vulnerable to retroactive interference. Wixted's review is instructive because the conception of a memory as something that could be consolidated or interfered with is quite distinct from the conception of activation invoked here. Activation decay in the context of temporal integration is considered to be a purely physical process, and states of activation are considered to be more akin to states of energy than to quantities of information. In this sense, activation decay is construed to function more like the cooling of coffee or radioactive decay than the forgetting of meaningful information. In this physical sense, activated states are not subject to the memorial processes involved in encoding, storage, and retrieval of information, and so are not subject to the mechanisms considered by Wixted that could make the decay rate time dependent. In the absence of specific reasons to suppose that activation decay does not follow a simple linear rate equation, we will develop the consequences of an exponential law for activation decay.

The Meaning of τ

The importance of identifying the negative exponential as the form of activation decay is that it associates proximity constraints in perceptual organization with a definite and specific theoretical construct, the activation lifetime, τ. τ has psychological entailments through the circumstance that, although it has the dimensions of time, and is literally an amount of time, it does not function only as a time interval. In physical contexts of exponential decay, decay lifetimes will satisfy an equation that specifies its parametric dependencies, $\tau = f(a, b, c, \ldots)$. f and its arguments are specified by the particular physics that obtains in any given instance. For example, the physics that leads to Newton's Law of cooling makes τ a function of surface area, heat capacity, and the heat transfer coefficient. In the same way, if activation decay in temporal organization is exponential, then there is some functional relationship for the activation lifetime. The central problem addressed by the empirical work is the identification of the arguments of this function.

The parametric composition of τ poses a difficult problem insofar as the construct of activation is not tied to a fundamental theory that makes reference to physical quantities. Nor is it clear at what level of description the parameters of τ should be conceptualized. In so far as τ exists at the intersection where distal event flux is transformed into meaningful and stable percepts, it potentially could be parameterized by any combination of neuronal, ecological, or environmental variables. To make sense of τ dependencies, we have looked to biology and botany, where scaling is a central issue in the composition and structure of living systems.

An observation of potential relevance to the formulation of τ parameters is that animals often display size-correlated variation in their anatomical form, physiology, and behavior. That such correlations exist is an issue in its own right, raising questions of how natural selection has fashioned animal bodies so that much about their structure and function is highly constrained by the single determinant of size (Niklas, 1994). The study of these correlations forms the field of allometry, first conceptualized in terms of development and the differential growth of body parts relative to overall body size (ontogenetic allometry; Pélabon et al., 2013), but later generalized to include both physiological and behavioral characteristics of adult animals (static allometry). Recently, allometry has been extended to nonbiological/botanical entities that have well-defined sizes, such as cities (Li et al., 2015).

In its most general form, allometry is concerned essentially with one kind of relationship; a power law of mass such that *animal property* $= a \times \text{mass}^b$. The animal properties that have this form of size scaling are diverse and include, for example, head size (anatomy), heart beat period (physiology), burst acceleration (behavior), and so on. Although all allometries are based on statistical correlations, the goal of allometry is not the demonstration of a significant correlation, but rather the measurement of the mass exponent, b.

The types of animal properties that enter into allometric relations typically have a physical basis, and this allows the exponents to be interpreted within physical frameworks. The focus of any interpretation begins with an inquiry into whether the exponent expresses geometric similarity or not. Geometric similarity serves as the definition of isometry in biological contexts and is regarded as a kind of null hypothesis in the interpretation of scaling exponents. Allometries refer just to scaling that cannot be explained by geometric similarity, and so they inevitably require the introduction of additional constructs and can drive theory building (West and Brown, 2005, being a notable example). It is in the physical interpretation of power law exponents that allometry goes beyond correlational analysis and becomes a theoretically productive field.

The scaling properties of τ may not be empirically accessible, in so far as activation decay is not experienced in temporally organized scenes. What is experienced are the products of temporal integration, gestalts, and these do not decay exponentially with increasing time between event arrival. Ordinary experience reveals that grouping strength is fairly invariant until the temporal gaps between events approaches the proximity constraint—a song played at 120 bpm does not necessarily generate a stronger sense of melodic contour and rhythmic pulse than when played at 90 bpm. Psychophysical evidence of tempo invariance in rhythmic pulse may be seen in Figure 2 in Etani et al. (2018), where it is shown that groove ratings of drum breaks are independent of tempo in the range 75 bpm to 150 bpm, where most music is played. Much of the psychophysical data presented in this article will provide further evidence for this observation. Nevertheless, the scaling properties of τ may be investigated indirectly through the scaling properties of proximity constraints. Proximity constraint magnitudes are functions of τ, and if τ satisfies an allometry, so too will proximity constraints.

Overview of the Experiments

An investigation into proximity constraint allometry requires that proximity constraints be measured with some precision, and for this reason, we have sought examples of temporal integration that are associated with an objective task. The requirement in task design was that it generate data that permit inferences about whether temporal flux is being perceived as a structured pattern or not. The experience of rhythmic pulse is especially opportune in this regard as it may be assessed through drumming or tapping performance, and such performances naturally generate a time series—a form of data that is uniquely susceptible to the formal analysis of precision, stationarity, and autocorrelation. A second form of temporal integration that may be assessed through an objective task is long-range apparent motion. Here, we used a variant of a methodology originally developed by Proffitt et al. (1988) to introduce precision in a probe placement task as an index of the vividness of curved apparent motion paths.

In the first study, proximity constraints for the experience of rhythmic pulse were inferred from the time series of drumming performances across a range of tempi. The principal difficulty encountered in this study was in locating the proximity constraint at the level of the individual. A detailed discussion of this problem is presented in the Appendix together with a review of strategies employed in a variety of previous investigations. Results are presented for both child and adult samples, and a general allometric law for proximity constraints in pulse is developed. This discussion is supplemented by the production of a second allometric law for drumming precision. A theory of scaling in drumming precision is proposed that makes the prediction that allometry in precision will only exist at slow tempi in the neighborhood of pulse constraints. A second experiment that assessed allometry in drumming precision at 120 and 60 bpm presents data consistent with the theory. The second content area of apparent motion is then introduced where the technique we developed for measuring precision in probe placement on illusory curved motion paths is described. Data are presented that show that precision in probe placement exhibits the same scaling laws as the coefficient of variation (cv) in drumming performance; allometry in the precision of probe placement exists, but only near the watershed SOA where the percept of apparent motion is difficult to maintain. The article concludes with a discussion of how the derived scaling exponents for proximity constraints might be interpreted, with particular attention paid to the forms of scaling that arise from energy exchange between animal bodies and their environment.

Experiment 1: Allometry of Rhythmic Pulse Proximity Constraint

In this study, drumming performances were recorded over a range of tempi. Individual performances were evaluated to determine the slowest tempo, or equivalently, the maximum time interval between beats at which any given person could produce a stable drumming performance. We will refer to this limiting interval as *t-horizon* in so far as it serves as a temporal horizon for the relatability of successive beats. Allometric relations were constructed for both *t-horizon* and for the coefficient of variation (cv = mean/standard deviation) defined on the time series of interbeat intervals. Both adults and children were assessed to extend the range of body size as much as possible. This led to an interpretation of the data that included both ontogenetic and static allometries, as the two groups produced similar but offset power laws. We present the results for adults and children separately and then combined.

Analysis of Slowest Stable Drumming Tempo in Adults

Participants

Fifty-eight adults participated in the study. The participants were students at the University of Texas at Austin between 18 and 30 years of age. Heights ranged from 58 to 77 inches. Participants were admitted into the study regardless of musical experience or training. The sample is objectively large so that all of the principal comparisons and regressions were statistically significant.

Procedure and Design

Drumming data were collected using a Roland Handsonic electronic drum that permitted highly accurate recordings of drum strikes via midi signals, as well as compelling auditory and tactile feedback to the participant. The Handsonic drum was configured to simulate the sound of a conga drum. Each participant provided drumming performances at eight tempi that were chosen to elicit both the feeling of rhythmic pulse, as well as the feeling of being lost. These tempi were 80, 70, 65, 60, 55, 50, 45, and 40 beats per minute, or equivalently, interbeat intervals of 0.75, 0.86, 0.92, 1.0, 1.1, 1.2, 1.3, and 1.5 s. In each condition, participants used their dominant hand to drum along to a metronome for approximately

Figure 2
Time Series of Interbeat Intervals Collected From Participant 71 in Experiment 1 in a Continuation Drumming Paradigm

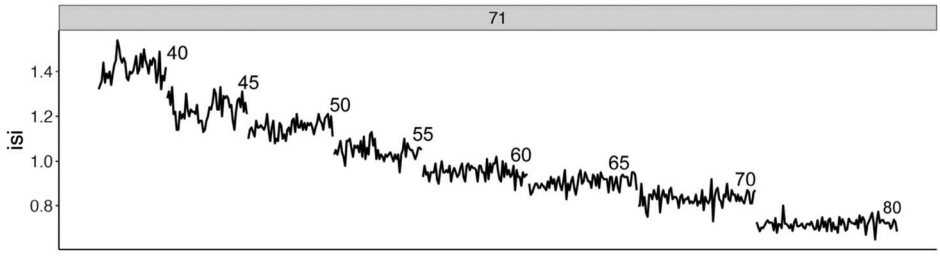

Note. Shown are performances at each of the eight tempi assessed. Plots such as these were used in the assessment of the slowest tempo where stable drumming was achieved.

10 s. Immediately after this practice period, the metronome was turned off, and the participant continued drumming for 60 s at the chosen tempo. This process was repeated until all eight performances had been collected. Height, age, and gender were also recorded from each participant. The ordering of tempo conditions was chosen to allow the participant to experience rhythm in the first performance, with the more difficult tempo conditions introduced subsequently: 80, 60, 50, 70, 45, 65, 40, and 55 bpm. Certainly, other orders might be contemplated, but this design served the purpose of giving people a mixture of experiences where they were occasionally lost without sacrificing the sense that their efforts were on the whole productive.

Analysis I: Visual Inspection of Time Series

The goal of the analysis was to estimate the slowest tempo at which individual participants could demonstrate a stable performance. The assessments were made just on the performance data, with no knowledge of any personal characteristics, such as height or gender. In so far as this study appears to be the first to attempt to determine the limits of rhythmic pulse on an individual basis, we undertook two independent evaluations of the performance data conducted by different people. In both cases, decisions about slowest stable tempo were made primarily on visual inspections of the time series of interbeat intervals, the rawest depiction of a drumming performance. Other methods that have been developed for determining *t-horizon* are reviewed in the Appendix.

The initial set of judgments used a plotting format where the eight performances were plotted separately but with common axis ranges and axis dimensions. The second set of judgments were made using a format where all of the time series shared a single frame. This second format was found to greatly facilitate time series comparisons at different tempi. An example from the second round is shown in Figure 2 for a participant with code 71.

An informal walk-through of how the slowest stable tempo for participant 71 was identified will clarify what is involved in this form of data analysis. This participant produced sequences of interbeat intervals that fluctuate but without substantial drift at tempi down to 60 bpm. The performance at 55 bpm does not drift, but the fluctuations appear to exhibit intermittency in amplitude. The performance at 50 bpm looks like it is beginning to generate some hill/valley structure. Hills and valleys dominate the performance time series contour at 40 and 45 bpm, evidence of random walking (see the Appendix for a discussion of random walking and the loss of rhythmic pulse). So, from the portraits, it would be concluded that the slowest stable performance is either at 50 bpm or 55 bpm, depending on how dispositive one regards intermittency as evidence of losing rhythm.

Additional statistics that speak to stability are measures of predictability (lag-1 autocorrelation) and precision (cv). The lag-1 autocorrelation is particularly useful here as a check on visual impressions of random walking. Formally, the lag-1 autocorrelation measures how predictable the ith interbeat interval is given the $(i - 1)$st interbeat interval. But practically, we are mostly interested in the circumstances when it is large and positive, and this will occur when the intervals form a contour dominated by hills and valleys. These statistics are shown in Figure 3 illustrates for participant 71.

An analysis of this participant's cv and lag-1 autocorrelation begins with the observation that all of the performances have cvs

Figure 3
Coefficients of Variation and Lag-1 Autocorrelations for Each of the Eight Tempi Assessed for Participant 71

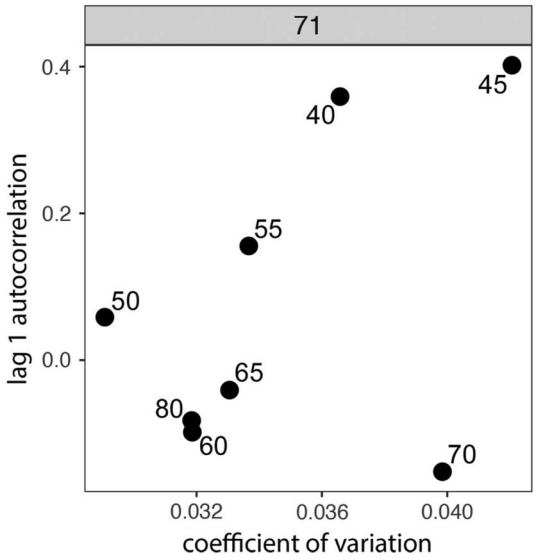

Note. These statistics were computed from the time series of inter-beat intervals and were used to supplement the assessment of the slowest achievable stable drumming.

smaller than .05, with a cluster around .035. Experience with measurement of stability characteristics of professional drummers has taught us that a cv of .03 is objectively small. Participant 71 is able to maintain relatively low variability even when the time series of interbeat intervals indicates random walking. More discriminating are the lag-1 autocorrelations. The performances at 40 and 45 bpm are positively autocorrelated and clearly more autocorrelated than the other performances. Large positive autocorrelation scores are symptoms of random walking, a feature already noticed in the time series portraits. (Negative autocorrelations observed at faster tempi arise from the circumstance that every drum strike both ends one interbeat interval and begins the next. The consequences of this coupling for autocorrelation are discussed in Gilden et al. 1995). The performance at 50 bpm has the smallest cv of any performance, and its lag-1 autocorrelation is smaller than the performance at 55 bpm. The overall impression from the statistics and visual inspection is then that the 50 bpm performance is a good candidate for being the slowest tempo at which this person can execute a stable performance, and given the temporal resolution of this study, this person has a *t-horizon* of 1.2 s.

Analysis II: Diffusion Rate Analysis of Time Series

The diffusion rate statistic Δ'(tempo), introduced by Madison (2001) and discussed in detail in the Appendix, provides a relatively independent method for inferring slowest stable performances. This statistic is constructed to take on positive values when the tempo of a performance diffuses away from the intended tempo and to take on values close to zero when the performance tempo is steady. As an instrument for inferring *t-horizon,* it functions best when there is a step discontinuity at one specific tempo. In that case, the position of the step specifies the slowest tempo at which a stable performance is possible. In practice, however, Δ'(tempo) may not be a step function of tempo, and settling on a value of *t-horizon* may entail some uncertainty. An example of what is involved in inferring *t-horizon* from Δ'(tempo) is shown in Figure 4.

Figure 4 shows Δ'(tempo) for participant 71 that person whose performances are depicted as a time series in Figure 2. Here, there is no step discontinuity in Δ'(tempo), and settling on a value of *t-horizon* comes down to an analysis of features in a sawtooth pattern. One feature which is particularly salient is the maximal diffusion rate at 45 bpm. The utility of this feature in assessing *t-horizon* would be enhanced were the diffusion rate at 40 bpm also large and positive, but instead it is large and negative.

Negative diffusion rates are inherently unphysical, insofar as diffusion processes tend to create separation over time and not convergence. In the spectral domain, a negative diffusion rate corresponds to a spectrum with greater power at high frequencies than at low frequencies, a circumstance typically encountered only in the spectrum of a difference process. In the case of participant 71, the negative diffusion rate at 40 bpm is an artifact created by sample size and by specific idiosyncratic structures that are observable in the original time series. In the first place, this tempo has the fewest number of interbeat intervals (in our methodology), so any statistic that characterizes performance at 40 bpm will be based on a relatively small sample size. The sample size issue is made more acute by the constraint that the number of samples that goes into the median estimate of drift, $|X(i)-X(i+w)|$, decreases with increasing window size, w [see the Appendix for the construction of Δ'(tempo)]. It also happens that this particular time series manages to wander back to the tempo where it embarked, ensuring that many of the estimates of absolute difference at large w will be small, hence the negative slope in $\Delta(w)$ with separation size.[3] Recognizing that the negative diffusion rate at 40 bpm is anomalous, it seems that the last low diffusion performance occurred at 50 bpm, and that value was chosen to mark *t-horizon*.

Figure 4
Madison (2001) Diffusion Rate Statistic Plotted for Participant 71

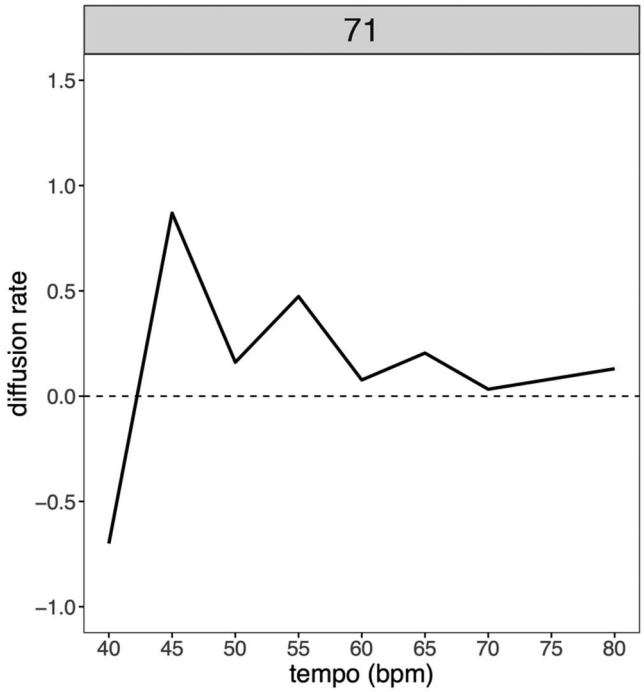

Note. This statistic provides a quantitative measure of the stability of any given drumming performance and serves as a check on the informal method of visual inspection.

Results

Figure 5 plots derived values of *t-horizon* versus participant height. Panel A shows the inferred values of *t-horizon* from both rounds of visual inspection of interbeat interval time series. The first

[3] Some perspective on the statistical problems inherent in diffusion rate analysis may be had by considering how variability is distributed across scale (w) in the calculation of diffusion rate. The general situation in time series analysis is that high frequency (small w) variation is always measured with lower variance than low frequency (large w) variation. The reason for this is due just to square-root-n statistics in standard errors of mean values. High-frequency (short wavelength) structure is resolved in smaller windows than low-frequency structure, and the availability of windows for computing averages will be greater where windows are smaller. In the present context, variability in estimates of $\Delta(w)$ increases with the size of w because the number of windows available for computing absolute differences decreases as the scale of separation, w, increases. In regression models of $\Delta(w)$ with w, the most poorly determined values of $\Delta(w)$ may exert considerable leverage, as they are located at a terminal end. This unhappy situation is encountered generally where model selection requires resolution of structure at low frequencies (Gilden, 2009).

Figure 5

Estimates of t-horizon, the Longest Interval of Time Between Successive Drum Beats That Could Be Bridged in the Production of a Stable Nonsynchronized Drumming Performance for a Population of Adult Participants

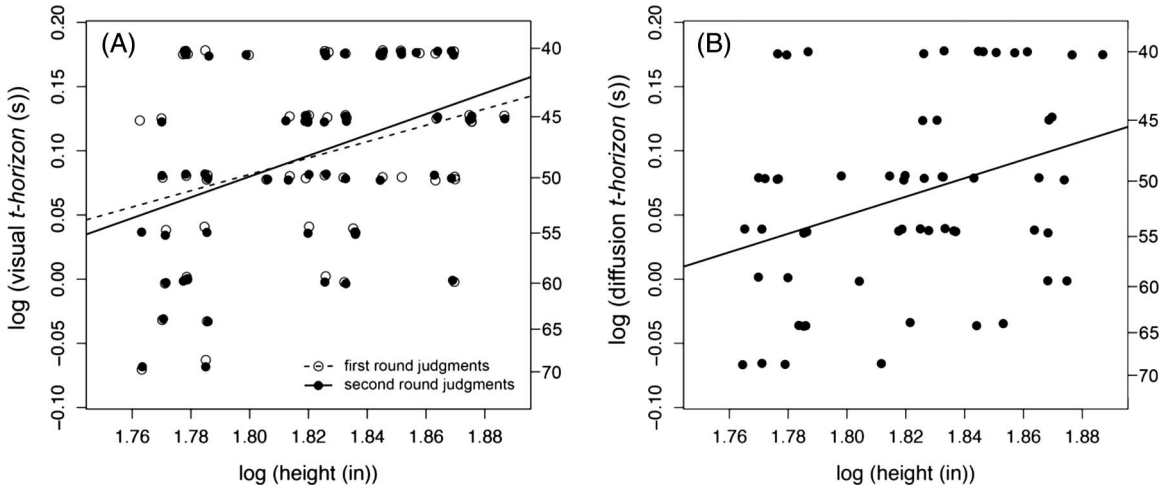

Note. Panel A shows regressions of *t-horizon* onto height for estimates deriving from two independent rounds of visual assessment of stability and meandering in the time series of interbeat intervals. Panel B shows regressions of *t-horizon* onto height for estimates derived from Madison's (2001) diffusion rate statistic. For clarity, a beat per minute scale (bpm) is also included so that it is clear where people achieve their slowest stable performances

round is plotted as unfilled circles, and the second as filled dots (jittered slightly to reveal overlap). It is evident that there is considerable overlap between the two rounds of *t-horizon* assessment. Of the 58 participants, there were only three instances where estimates of *t-horizon* differed between the two rounds. Panel B shows inferred values of *t-horizon* from diffusion rate functions of tempo (also jittered).

In both panels of Figure 5, height and *t-horizon* are plotted in the log–log plane, the traditional format for regression analysis in the field of allometry, as allometric relations are typically expressed as power laws of body size. Linear regressions were computed in this plane so that the slope gives an estimate of the power law exponent. The principle distinction between visual assessment and diffusion rate analysis in the assessment of *t-horizon* is in overall criterion setting, manifest as intercept shifts in the regression lines. Estimates of *t-horizon* made on the basis of diffusion rate are generically more conservative, smaller in magnitude (larger in bpm), than estimates made on the basis of visual assessment of diffusion.

The three sets of *t-horizon* judgments led to slightly different slope estimates that were nevertheless equivalent within the standard errors. The first round estimate of slope was 0.64 ± 0.24, $t(56) = 2.62, R^2 = .11, p = .006$, while the second round produced a slightly steeper slope estimate of 0.81 ± 0.24. $t(56) = 3.36$, $R^2 = .17$, $p < .001$. (All comparisons in this article are reported as one-tailed, as all of our hypotheses are one directional; allometries in biology generally associate longer time periods with larger animals.) The diffusion rate estimate of slope was 0.72 ± 0.27, $t(56) = 2.72, R^2 = .12, p = .004$, roughly at the midpoint of the two rounds of visual inspection. These results are summarized as the production of a consistent measurement of the power law exponent using two independent methods of analysis, in addition to two different rounds of visual inspection.

Analysis of Slowest Stable Drumming Tempo in Children

In the development of allometric laws, there are both statistical and scientific reasons to assess the widest range body sizes possible. Statistically, there is the concern that restriction of range will attenuate correlations, and this in turn will lead to systematic errors in the calculation of power law exponents. Restriction of range may be an issue in our first study, as the smallest person was about 58″, and the entire height range spanned only 19″. Scientifically, it is of interest to establish whether scaling exponents are different in different regimes of body size. Although we are not interested in conducting a developmental study of rhythm, it is the case that children do provide a pool of relatively short participants, and for both of the reasons given, it is of interest to include their *t-horizons* in a more inclusive and broader examination of allometry.

The costs to including children are twofold. First, the participation of children introduces age as a confounding variable—age and body size are correlated in children. Second, whatever height relation may be found in temporal horizons in children, it cannot be easily interpreted in terms of allometry. Allometry, as has been historically practiced, applies to the differential growth of body parts during development of single animals (ontogenetic allometry) or to relations between somatic/behavioral properties and body size across different adult animals (static allometry). An assessment of the type undertaken here is not ontogenetic because it is not longitudinal, and it is not static because our child participants are at different stages of incomplete development. With these cautions, we report on what children of different sizes can achieve in rhythmic expression at slow tempi.

This study replicates the adult study in every detail except (a) the 45 participants ranged in age from 6 to 12 and were recruited mainly from the afterschool care program of St. Andrew's Episcopal School in Austin, TX and (b) due to limitations in attentional vigilance, we

recorded drumming for 15 s per tempo condition instead of for 1 min. This group substantially removed the restriction of range in height (extending the range down to 45″), but the shorter sequence lengths necessarily make the determination of slowest stable tempo more ambiguous. As with the adults, we report two separate sets of judgments by independent observers, where the second round again incorporated integrated time series plots of the type shown in Figure 2, as well as cv/lag 1 autocorrelation plots of the type shown in Figure 3. The first round employed only individual time series plots. Both sets of assessments were made with no knowledge about the participants except that they were children, which was clear in any event from the shorter sequence length.

The results of this study are shown in Figure 6 as two height regression models of *t-horizon*, corresponding to the two sets of independent assessments of *t-horizon*. Again, the plots are rendered in the log–log plane, so that slopes may be interpreted as power law exponents of height. The two assessments generated highly concordant slopes. First round *t-horizon* assessments (open circles) yielded a slope estimate of 0.91 ± 0.28, $t(43) = 3.22$, $R^2 = .19$, $p = .001$, while second round assessments (filled dots) yielded the slope estimate 0.83 ± 0.21, $t(43) = 3.92$, $R^2 = .26$, $p < .001$.

The vertical displacement of the two fitting functions reflects the circumstance that the two rounds of *t-horizon* assessment differed in strictness on their stability criteria, the second round being somewhat more conservative in setting a criterion for what constitutes a stable performance. Practically, this means that the two judges might disagree about whether a wobbly performance reflects normal Weberian growth error or whether it represents random walking. Criterion differences aside, the power law exponents derived from the two sets of *t-horizon* assessment are identical within the errors. The implication is that assessment of *t-horizon* on short-time series can be done with some systematicity, but that it is more sensitive to criterial variation than assessments of the longer sequences analyzed in the adult population.

Figure 6

Estimates of t-horizon for a Population of Child Participants

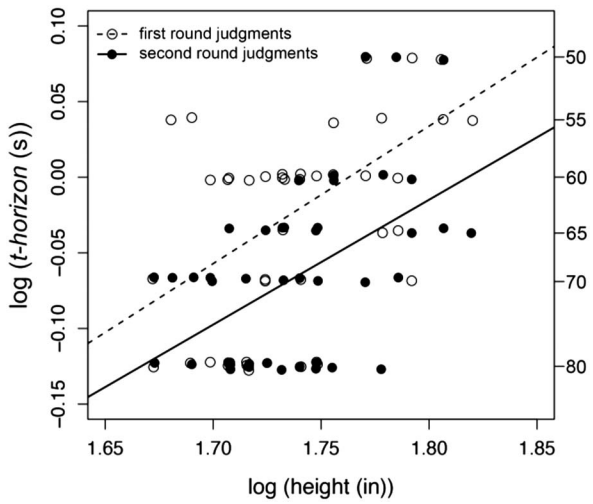

Note. Shown are regressions onto height for estimates deriving from two independent rounds of visual assessment of stability and meandering in the time series of interbeat intervals. A beat per minute scale (bpm) scale is provided for reference.

The issue of how variation in *t-horizon* should be interpreted within a developing population is not straightforward insofar as age and height are naturally highly correlated; the correlation in our sample is .8, and either or both could be relevant. As allometry has not been an issue in any previous study of rhythmic pulse, it is not surprising that, in large developmental studies of rhythmic abilities in children and adults (McAuley et al., 2006; Drake et al., 2000), only age was considered as a factor. However, in our sample of children, it is height specifically that appears to be driving the variation in *t-horizon.* Focusing just on the second set of judgments, in simple regressions (not log-transformed) on single variables, age alone explains 18%, $t(43) = 3.07$, $p = .002$, and height alone explains 28%, $t(43) = 4.05$, $p < .001$, of the variation in *t-horizon.* Multiple regressions focused on unique variance (Type III sums of squares) clarified the respective roles of these two variables. When height and age are both retained as predictors, the combined model does not exceed that of height alone; height still acts as a significant predictor, $t(42) = 2.36$, $p = .01$, while age does not, $t(42) = .046$, $p = .48$. In the context of model selection using the Akaike information criterion (AIC) in a stepwise regression, the AIC value for a height-only model is exactly two smaller than a height plus age model; adding age has no effect on model fit, but it does add a model parameter. The statistical conclusion here is not that development is unimportant in setting *t-horizon* but that developmental effects are expressed through height.

Global Analysis of *t-horizon*

The finding that height effectively parameterizes *t-horizon* for both children and adults suggests that the two data sets be merged into a single analysis. In Figure 7, we display the entire set of *t-horizon* assessments (2nd round assessments only) as a function of group and height, together with their individual regressions. The individual regressions (shown as dashed lines) have similar slopes (adults = 0.81, children = 0.83), but the intercepts are clearly differentiated. These observations motivated a global regression model over both groups that had three free parameters; one slope and two intercepts. Such a model is formally what is constructed in an ANCOVA, although ANCOVA is typically used for the purpose of hypothesis testing about group differences where there is a covariate. Our purpose here is simply to fit the merged assessments of *t-horizon* with a model that incorporates the information gained from the separate child and adult regressions.

The common slope in an ANCOVA model is 0.82 ± 0.16, $t(100) = 5.02$, $p < .001$, and the intercept difference is 0.1, $t(100) = 5.38$, $p < .001$. A simple regression, shown as a solid line, has also been fit to these data. As a simple regression cannot capture group intercept differences, it fits a much steeper regression line, $b = 1.47$, $t(101) = 12.0$, $p < .001$. In terms of R^2, it is arguable that ANCOVA provides a better statistical description than a simple regression over the entire combined population. An ANCOVA model captures 68% of the variance in *t-horizon,* while a model with a single intercept captures 59%. Even with the additional intercept in the ANCOVA, the difference in AIC values between the two models is 24, with an evidence ratio in excess of 10^5.

A final point concerns whether these studies provide an adequate picture of *t-horizon* variation. In this regard, although the addition of children into the study adds some complexity both in measurement and interpretation, the effort did succeed in providing better height

Figure 7

The Entire Collection of Second Round Visual Estimates of t-horizon Regressed on Height for Both Children and Adults

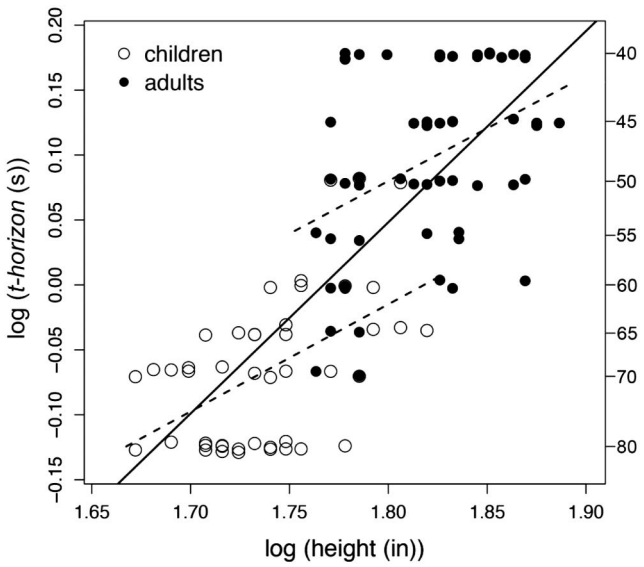

Note. A simple regression over the entire participant population is shown along with separate group regressions. A beat per minute scale (bpm) scale is provided for reference.

coverage and greatly extended the range of measured values of *t-horizon*. The combined child/adult sample resolved a 0.75 s range in *t-horizon* (40 to 80 bpm), an ecologically meaningful differential, as the nominal maximal value (built into metronomes) of *t-horizon* is 1.5 s.

Some perspective is required here to appreciate the role that height is playing in *t-horizon.* Although perhaps obvious, it is the case that the measurement of *t-horizon* is not embedded in well-established and well-understood psychophysics. It does not reflect some aspect of, say, early vision where there are sophisticated measurement techniques that are supplemented by extensive physiology and quantitative theory. Rather, *t-horizon* is the watershed for a particularly abstract aspect of human experience, a temporal dividing line between the experience of rhythmic pulse and the experience of beats separating into a stream of isolated moments. And furthermore, there is no established psychophysics for its measurement. In this light, the demonstrated impact of height on *t-horizon* is quite extraordinary. These regressions are performed on raw data, there is no averaging prior to model fitting, and yet, height models with only two (simple regression) or three free parameters (ANCOVA) account for upward of 60 to 70% of the variance. To put these proportions into context, experimental designs in cognitive psychology, especially those employing speeded forced choice, typically contend with large amounts of unexplained variability (Gilden, 1997, 2001, 2009). Much of cognitive theory is based on methodologies where only 10% of the total variability reflects the experimental design.

ANCOVA Models of Allometry

ANCOVA models often arise in the development of allometries when more than one identifiable group is regressed onto body size. In the analysis of the Kleiber Law, for example, Heusner (1982) employed ANCOVA to allow for intercept shifts between various species of mammal. In our study, the groups are defined simply by the child/adult distinction, a distinction that succeeded in extending the height range but also succeeded in introducing an intercept shift. Although children and adults do not represent two different species, they do represent different stages of development, and the existence of an intercept shift may be explained in terms of the distinction between ontogenetic and static allometry. In Figure 8, we illustrate how a mixture of incomplete developmental trajectories could easily yield an intercept shift relative to a static allometry realized in adults.

The filled circles represent the measurements made in the adult study, and the regression line represents the static allometric law relating height to *t-horizon*. The open circles represent the child data. Each child is depicted as being on a different ontogenetic allometric trajectory corresponding to their unique growth pattern and to the adult size that they will eventually achieve. These trajectories were not measured by our study, in so far as our study was not longitudinal, capturing each child once at a particular state of development. Nevertheless, it may be presumed that individual ontogenetic trajectories eventually attach to the adult static allometry, again according to the unique growth pattern of each individual. Any height law that is discovered within snapshots of the ensemble of developmental trajectories is a pseudoallometry, reflecting neither a developmental trend nor an asymptotic trait scaling. In this picture, the intercept shift arises from the circumstance that the ontogenetic trajectories are steeper than the static allometry (see Pélabon et al., 2013) and from the fact that the children have not yet attached to the asymptotic static law that marks the end of development. The positive slope of the pseudoallometry arises then from the general patterns in both the (theorized) ontogenetic and (empirically validated) static allometries, where larger body size is associated with larger values of *t-horizon*.

Figure 8

A Model Depicting how the Ontogenetic Allometry in a Developing Population and a Static Allometry in an Adult Population Could Together Create the Conditions Where an ANCOVA With an Intercept Shift Would Be Required to Interpret the t-horizon Data in Experiment 1

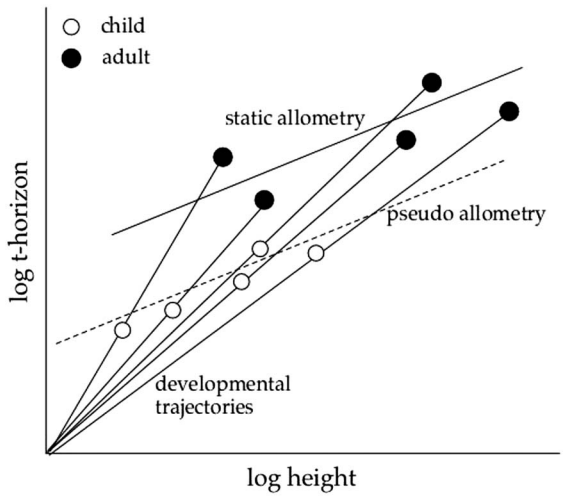

Motor Contributions to *t-horizon* Allometry

In view of the fact that this is an originating study of the existence of allometry in a proximity constraint, there is a concern that these results might be artifactual or trivially explained. We consider here two physical aspects of drumming performance that might be conjectured to create body size relations in rhythmic proximity constraints. One mechanism that deserves comment has to do with motor delay in the actuation of a drum strike. There are obvious motoric aspects to drumming that are peripheral to cognitive timing process, and some of these do scale with body size. Motor delays enter the Wing–Kristofferson model of rhythmic drumming (Wing & Kristofferson, 1973) as an additive factor (M_i) that offsets the moment of the ith drum strike (I_i) from the internal sense of beat placement (C_i); $I_i = C_i + M_i$. M_i might satisfy an allometry, in that larger people have greater body-crossing times for neural conduction, and in fact, a height$^{3/4}$ law has been proposed (Lindstedt & Calder, 1981)—an exponent quite consistent with the *t-horizon* regressions reported here. The contribution of neural conduction to *t-horizon* allometry may be estimated by considering the observed range of height variation. Height differences in our participant population had a range of ½ m, translating to about a 10 ms range of difference in neural transmission times for a presumed conduction speed of 50 m/s (Macefield et al., 1989; Thomas et al., 1959). A 10 ms of slack is small compared to the 750 ms range covered by *t-horizon,* implying that scaling of neural transmission cannot substantially contribute to scaling of *t-horizon.*

Motor delays also arise from hand lowering to the drum surface, but there are several reasons to reject hand lowering in drumming as a pathway to allometry. First, the geometry of drumming is not size scaling. People who are taller do not hold their hands further above a drum surface than people who are smaller; everybody holds their hands a couple of inches above the drum surface. Second, drum strikes are ballistic, percussive, events, and are not executed at the natural frequency that arms execute, say, while swinging during walking motion. Natural arm frequency is size scaling, but pendular motions occur over timescales of seconds; a percussive hand strike consumes much less than a second. A very liberal estimate of the time elapsed for a percussive hand strike places the hand about 10 cm above the drum surface and being lowered at 1 m/s. In this case, the hand lowering time is about 100 ms, not in the same regime as pendular period, and again, too small to be relevant to the observed range of *t-horizon*.

Finally, we wish to stress that whatever influence height has on the physical execution of a drum strike that influence is tangential to the breakdown of rhythmic pulse that invariably occurs at sufficiently slow tempo. Losing pulse is not a motor problem; it is a knowledge problem—not knowing where to place a drum strike in a context where drum strikes are in fact either on the beat or off the beat. What *t-horizon* captures is the critical tempo where people transit from knowing where to place drum strikes to not knowing. The onset of random walking at slow tempi is evidence of a cognitive struggle, attempting to place drum strikes on beats when rhythmic pulse has been lost. The tempo at which this happens is not linked in any obvious way to the body, yet it manages to satisfy an allometric relation. Somehow, a transition in knowing is linked to body size. That is what must be explained.

The influence of a Proximity Constraint on Drumming Precision

There is considerable evidence that Weber's Law holds for the rhythmic production of temporal intervals, in the sense that cv is generally observed to be constant across a substantial range of tempi (also referred to as a scalar property of timing—see Wearden 1991). McAuley et al. (2006), for example, showed that adults (older than 18) in a continuation tapping task have remarkably constant cv's of about .06, extending over a range of interbeat intervals from 150 to 1,700 ms. Similar data were reported by Madison (2001). McAuley et al. also find that children obey a modified Weber's Law; children older than about five have a fairly constant cv that increases slowly with decreasing tempo, but the absolute value of that cv increases with decreasing age.

Violations of Weber's Law at Slow Tempi

To provide context for an investigation into cv allometry and to make contact with previous investigations of rhythmic performance, we display in Figure 9 group averaged cv (<cv>) as a function of tempo, split between children at two age groups (a median split) and adults. The displayed trends in <cv> are in broad agreement with McAuley et al. (2006) over the common range of tempo assessment; adults show fairly constant values out to 60 bpm, and children, especially the youngest, display relatively larger <cv> values that increase more dramatically with decreasing tempo. <cv> values in the two studies are also generally in numerical agreement in the child sample, but our adult <cv> values are systematically smaller than

Figure 9

Group-Averaged Coefficients of Variation (cv) as a Function of Target Tempo for Three Groups Assessed in Experiment 1: Adults, Children 9–14, and Children 8 and Under

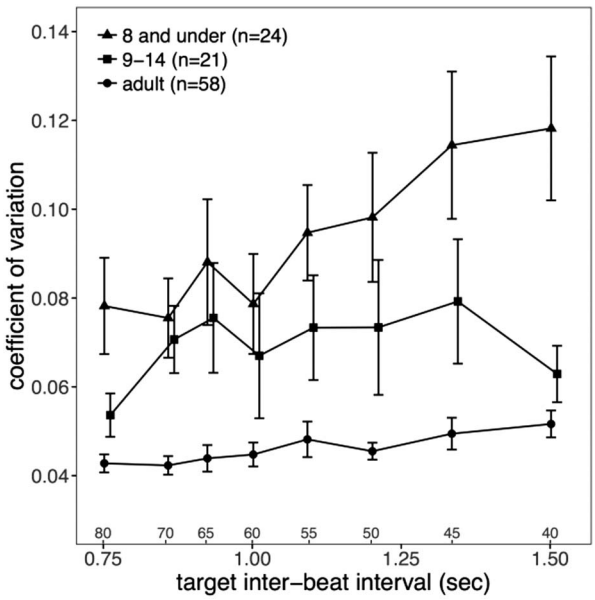

Note. Error bars depict standard error of the mean. Flat functions, as observed in the adult group for tempi faster than 60 bpm, indicate the Weberian property where error growth is proportion to the magnitude of the quantity produced, in this case an interbeat interval.

McAuley et al.'s by about 20%. We do not have an explanation for the superior adult performance in our study except to note that performing on a Roland Handsonic drum surface with headphones providing conga auditory feedback may be a more compelling experience than tapping on a copper plate (see methods section in McAuley et al.). We also do not have a satisfactory explanation for the relatively low <cv> at 40 bpm in the 9–14 age group. A <cv> value close to .06 in this group is an unusual achievement and suggests that some of our participants were subdividing the interval through some artifice we did not detect, perhaps subvocal counting.

Figure 9 makes clear that Weber's Law is substantially violated in our study. This outcome was expected as the design focused on performances at largo tempi (40–60 bpm) so that *t-horizon* could be estimated. Our account of the observed violations of Weber's Law begins with the observation that drumming performances display greater precision when the performer is experiencing rhythmic pulse than when they are not. It is inevitable that non-Weberian drumming will be observed at tempi where people have lost pulse—at tempi slower than the watershed tempo associated with their *t-horizon:* 60/*t-horizon*. In general, stable drumming performances at tempi > 60/*t-horizon* typically generate cv values in the range .04 to .06, while meandering performances at tempi < 60/*t-horizon* typically generate larger cv values associated with tempo diffusion. (Technically, cv is only well defined on stable performances. Meandering performances are nonstationary, and cv values will depend on the sequence length. This makes the numerical values associated with <cv> growth difficult to interpret.) The growth of <cv> with decreasing tempo of assessment occurs because <cv> is a group averaged statistic, and at any given tempo of assessment, some people may be experiencing rhythmic pulse while other are not—this is a consequence of the allometry in *t-horizon.* Consequently, the <cv> values in Figure 9 reflect mixtures of stable and unstable performances where the mixing proportions vary with tempo of assessment. <cv> grows as tempo of assessment decreases because the proportion of people who have lost pulse increases. <cv> will be constant only in tempo regimes where there are no meandering performances added into the mix, and this occurs in the adult population at tempi faster than about 60 bpm.

Theory of cv Allometry

These same considerations also imply that cv might satisfy an allometry in slow tempo regimes as a consequence of the more fundamental allometry in *t-horizon*. This textbook example of regression effects is illustrated in Figure 10. In this figure, the allometry in *t-horizon* is depicted to reflect the general trend that taller people encounter their proximity constraint in rhythmic pulse at slower tempi. Centered on the regression line about the predicted values are residual distributions of *t-horizon*. For illustrative purposes, homoscedasticity is assumed so that these distributions appear as invariant with height.

Consider then a tempo, *T*, where a cv assessment is conducted. This tempo is illustrated as a solid horizontal line that cuts the various residual distributions at different *z*-scores. Within each residual distribution, people whose *t-horizon* tempo is slower than *T* will contribute stable, low cv performances. This group is illustrated as the shaded region in the residual distributions that extends from *T* and continues towards slower tempi. Everybody else in the residual distribution is attempting a performance at a tempo

Figure 10

Theory of Allometry in the Group Averaged Coefficient of Variation

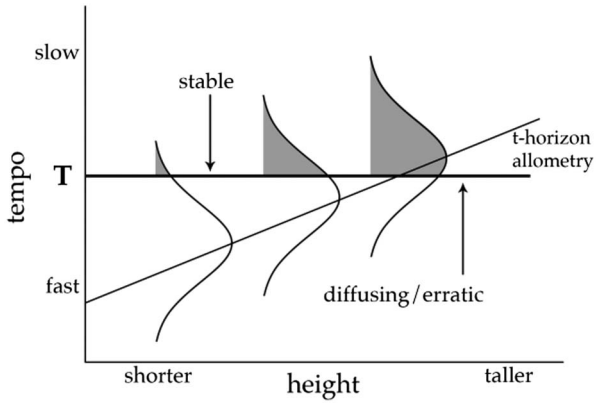

Note. At a given sufficiently slow tempo of assessment (*T*), each height subpopulation will have a mixture of stable (low coefficient of variation [cv]) and unstable (large cv) performances with proportions that vary with height. The dependence of relative proportions on height creates cv allometry.

(*T*) which is slower than their *t-horizon* tempo, and consequently, they contribute large cv, diffusing performances. In the illustrated example, the left most residual distribution is dominated by people contributing diffusing performances (least shaded area), while the rightmost distribution is dominated by stable performances (most shaded area). The allometry in shading proportion immediately translates to allometry in cv. This picture also suggests that there should be an entire range of tempi where no allometry in cv is observed. If the tempos of assessment were shifted downward in Figure 10 to a sufficiently fast tempo, all of the residual distributions would be completely shaded—the number of people contributing diffusing performances would be quite small. At such tempi, the differential shading of the residual distributions with height would not occur, and consequently, height would cease to be a factor. This is a testable proposition and will be examined in Experiment 2.

The argument that both allometry in cv and departures from Weberian growth of error in <cv> arise from the mixing of stable and unstable performances depends critically on the details of cv variation in these two regimes. To highlight the stable/unstable distinction in cv magnitude, Figure 11 plots all of the cv values that were assessed for all participants at each of each of the eight tempi in the design in terms of tempo distance from each participant's tempo of *t-horizon* (60/*t-horizon*). So, for example, a given cv assessed at 60 bpm would have an x coordinate of +10 if the person who produced that cv had a tempo of *t-horizon* measured at 50 bpm but would be plotted at −10 if that person's tempo of *t-horizon* was measured at 70 bpm. As positive x values correspond to performances where the tempi of assessment were faster than the tempi of *t-horizon*, cv values in this regime reflect predominantly stable performances. Negative x values refer to tempi of assessment that were slower than the tempi of *t-horizon,* and this marks the regime of unstable performances. $x = 0$ in Figure 11 marks the boundary between stable and unstable performances.

Figure 11 makes the obvious but important point that assessments of drumming precision depend critically on whether the performance is stable or whether it is diffusing or erratic. For $x > 0$, people

Figure 11

The Entire Ensemble of Coefficients of Variation (cv) Collected in Experiment 1

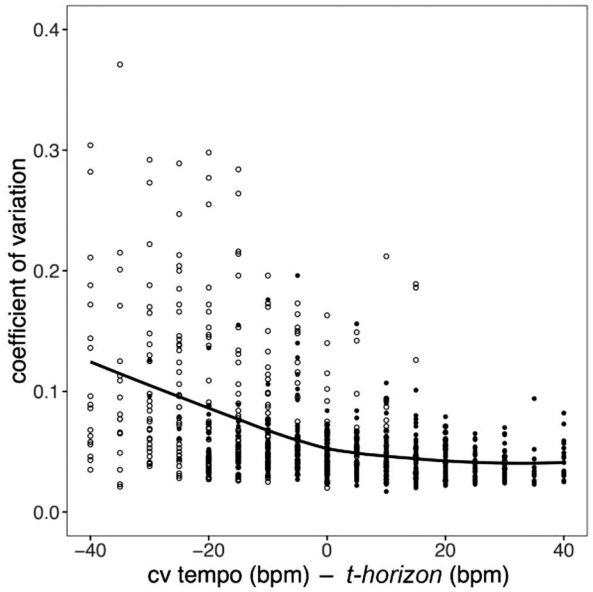

Note. Each person contributed eight values of cv, and these are plotted at tempi relative to the tempo associated with that person's *t-horizon*. Positive values indicate cv assessments in regimes of stable drumming performance, while negative values indicate assessments of performances marked by meandering or other erratic behavior. Open dots show cv values collected from children, while filled circles show adult cv values.

are producing stable time series, presumably because they are experiencing successive beats in relation to one another and the attendant emergent property of rhythmic pulse. The interpretation then is that for $x > 0$, cv is a measurement of a cognitive capacity, the feeling of rhythmic pulse, and Figure 11 shows that the ensemble of cv values in the stable regime is characterized by three features: cv is relatively small (about .05), cv is relatively constant across the tempo where it is assessed (the Weberian property), and cv values are relatively homogeneous across the entire population. None of these features are found in the ensemble of unstable performances located in the half plane $x < 0$. When the tempo of cv assessment is slower than the tempo of *t-horizon*, cv does not reflect the guidance of temporal organization, but rather the guidance of whatever strategies or knowledge can be used to decide when to strike the drum, given that the sense of target tempo has been compromised or lost. These strategies are evidently executed with a highly variable degree of accomplishment, leading to a high degree of heterogeneity in the cv values in Negative × Portion of Figure 11, especially in the child population. It is evident then that cv has the requisite structure to display allometric scaling, simply because the relative proportions of stable and unstable performances follow the allometry of *t-horizon*.

Empirics of cv Allometry

Exponents of cv allometries were computed at each of the tempi employed in the assessment of *t-horizon,* as regression slopes of log(cv) by log(height). Figure 12 shows these calculations as separate tracks for the child and adult samples. Error bars represent standard errors of the estimated slope. R^2 values are also included for each regression. It is evident that that cv scaling is fairly generic in both data sets; at all tempi slower than 70 bpm, negative exponents were statistically resolved ($p < .05$).

This result in itself has significant practical implications, in that cv is derived from rote calculation, while the derivation of *t-horizon* invariably involves some degree of judgment. As either variable can be used to demonstrate the existence of an allometry, the principal finding here, that proximity constraints in rhythmic pulse obey an allometric law, is freed from the complexity of measuring *t-horizon*. However, it must be stressed that the allometry describing *t-horizon* is the fundamental relation. In this framework, *t-horizon* is related to a tangible property of the memory system that mediates temporal integration, the activation lifetime. cv, in contrast, is a behavioral achievement with an allometry inherited from the circumstance that *t-horizon* creates a height trend in the mixing proportions of low cv stable performances and high cv diffusing performances.

The tempo variation in the cv exponents [slopes in the log(cv), log(height) plane] was not predicted, although some aspects of it are explicable in terms of the theory outlined so far. Taking Figure 12 at face value, cv exponents in the adult group are relatively constant near −1.4, while exponents in the child group become quite negative, in the neighborhood of −4. This difference is attributable to both the relative proportions of participants that are lost (randomly walking or otherwise executing erratic performances), as well as to the character of erratic performances. In the adult sample, as the tempo decreases, the proportion of people that are lost slowly increases, and those that

Figure 12

Slopes From Simple Regressions of the Coefficients of Variation Against Height in the Log–Log Plane as a Function of Tempo of Assessment for Both Children and Adults

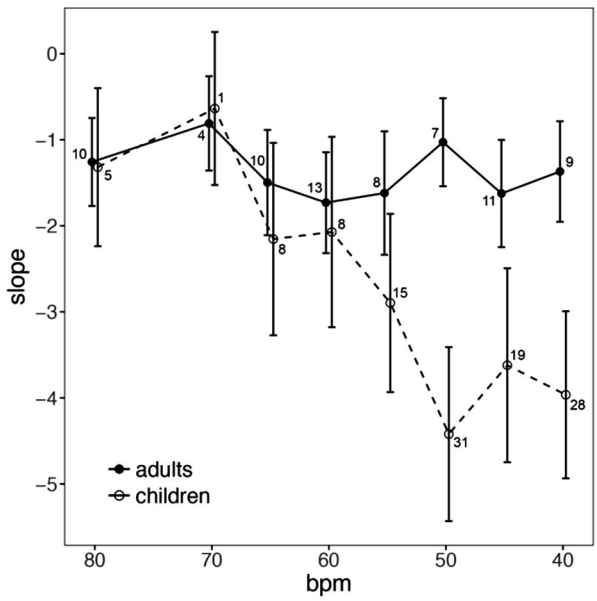

Note. Error bars depict standard error of the slope estimate. These slopes may be read as exponents of a power law allometric relation. Inset are proportions of variance explained by the regression—R^2.

are lost do not appear to be generating performances that are highly erratic. Referring back to Figure 9, we see that <cv> never exceeds .055 in the adult group and that the error bars are of relatively constant magnitude. The implication is that diffusing performances produced by adults are constrained in their wandering. In contrast, Figure 9 also make clear that <cv>, in both magnitude and variability, increases markedly with decreasing tempo in the child group, especially among the younger/shorter children. The stratification in <cv> that occurs in the median split in age in Figure 9 ends up being reflected in steep slopes in log(cv) regressions on log(height).

The correlation between age and height that exists generally in any child sample muddles the interpretation of cv scaling, as it did the interpretation of *t-horizon* scaling. In so far as it appears that cv allometry is a consequence of *t-horizon* allometry, it is plausible that, if height controls *t-horizon,* then it must also control cv. This turns out to be true, and the evidence is given in Table 1, where AIC and R^2 values are reported for regression models of cv based upon age and height, height alone, or age alone. These models were computed on the raw data (not log-transformed), to more easily interpret the relationship between the nested models (consequently proportions of variance will be slightly discrepant from Figure 12, which employed log-transformed variables). From an AIC point of view, age alone models are never preferred to height alone models, and adding age to height in a combined model never improves the goodness-of-fit. A study more focused on development than ours might find a more prominent role for age, but for our sample, the variation in cv is best explained as a function of height alone. This is the same conclusion we reached for *t-horizon*, and it motivated a global analysis of cv based only on height.

To generate a global model of height variation in cv, we focused on a range of tempi where both the cv scores themselves and the regression slopes with height in the children's data were relatively constrained (and perhaps more meaningful). From Figure 9, it appears that gross violations of Weber's Law appear in the youngest children beginning at 55 bpm, and this is also where the regression exponents become increasingly negative in Figure 12. Consequently, we defined a tempo averaged cv, denoted as cv*, over the four tempi, 60, 65, 70, and 80 bpm. Figure 13 shows height regressions of cv* for both adults and children.

Table 1
Comparison of Models With Age and Height, Height Only, and Age Only as Predictors for the Coefficient of Variation of Child Drumming Performances

	Age and height		Height only		Age only	
Tempo	R^2	AIC	R^2	AIC	R^2	AIC
40	27.1*	−123	27.0**	−125	19.1**	−120
45	17.4*	−107	17.0**	−109	8.4*	−104
50	22.5*	−115	22.2**	−117	12.1*	−111
55	18.7*	−137	18.4**	−140	9.8*	−135
60	7.5	−123	6.4*	−125	2.0	−123
65	6.5	−117	6.2	−118	1.3	−116
70	2.5	−158	2.0	−159	0.5	−150
80	3.2	−150	3.0	−152	2.6	−152

Note. For combined model, significance corresponds to the height term, as age was never significant when height was included as a term. AIC = Akaike information criterion.
* $p < .05$, one-tailed. ** $p < .01$, one-tailed.

Figure 13
Separate Regressions of the Tempo Averaged Coefficient of Variation, cv, Against Height in the Log–Log Plane for Children and Adults*

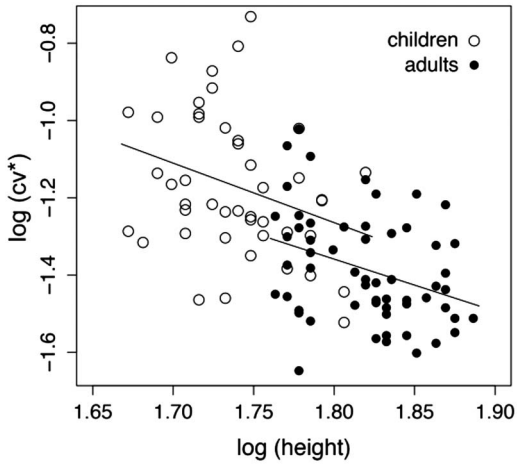

Note. The similar slope and manifest intercept difference motivated an ANCOVA model of these data.

Our analysis of cv* closely follows the analysis of *t-horizon* in detail. Regressing log(cv*) on log(height) in the separate groups produced results consistent with separate regressions at the four tempi that went into the average (see Figure 12). In the child group, log(cv*) was significantly correlated with log(height) [$b = -1.65 \pm 0.73$, $t(43) = -2.26$, $R^2 = .09$, $p = .01$], while log(age) was not [$b = -0.33 \pm 0.28$, $t(43) = -1.15$, $R^2 = .03$, $p = .13$]. Furthermore, adults were found to satisfy a static allometry [$b = -1.35 \pm 0.50$, $t(56) = -2.71$, $R^2 = .11$, $p = .005$]. As the slopes in the two groups were not statistically different, we again constructed an ANCOVA model with one common slope and two intercepts. In the ANCOVA model, the common slope is -1.48 ± 0.42 ($t(100) = -3.50$, $p < .001$), and the intercept difference is -0.095 ± 0.046 ($t(100) = -2.06$, $p = .02$). An ANCOVA explains 38.2% of the total variance, while a simple regression through both data sets explains 35.6%, a meaningful but recognizably marginal difference. The differential [AIC(ANCOVA)—AIC (simple regression)] = −2.29, leading to an evidence ratio in favor of the ANCOVA of about 3 to 1. This is not conclusive support for the ANCOVA, but it is worth noting as the two models select substantially different exponents. A simple regression model does not recognize an intercept difference and fits the data with a much steeper exponent ($b = -2.13 \pm 0.29$, $t(101) = -7.47$, $p < .001$) than the ANCOVA model. The principal conclusions then are that (a) drumming precision at slow tempi obeys an allometry and (b) the allometry in a tempo-averaged cv appears to have a structure similar to that of *t-horizon*—a pseudoallometry in developing children and a static allometry in adults.

Experiment 2: Allometry in the Coefficient of Variation at Fast and Slow Tempi

Our interpretation of cv scaling is that it is an inherited property from *t-horizon* scaling and that cv scaling might be limited to tempi where people are substantially divided in terms of whether they are

able to produce a stable, low cv performance. It is a prediction of the framework shown in Figure 10 that cv scaling should not occur at sufficiently fast tempi. If everybody is contributing stable performances, the fact that *t-horizon* is scaling ceases to be relevant. In particular, there is no prediction that height plays a scaling role at tempi where music is typically played, in the range 90 to 160 bpm. Culturally, there is no reason to suspect that size conveys any advantage in musical performance. Solid drumming performances seem to be a universal property in human populations.

This prediction could not be directly addressed using the data collected in Experiment 1, as the design was deliberately constructed to efficiently measure a proximity constraint for rhythmic pulse and the tempo conditions were chosen to be challenging. In Experiment 2, we determine whether there is allometry in cv at a tempo more in alignment with drumming tempo preference. As 120 bpm is typical of the tempo chosen by adults when asked to spontaneously execute a drumming performance (McAuley et al., 2006), this tempo was chosen for one of the conditions in Experiment 2. This condition would suffice to test the conjecture that cv scaling is limited to the neighborhood of *t-horizon,* but as this report is the first in the literature to find cv scaling at any tempo, a 60 bpm condition was also included simply to test the reliability of a key finding.

In this study, 43 participants, all adults between 60 and 76 inches, engaged in a continuation drumming task at 60 and 120 bpm. As in Experiment 1, we used a Roland Handsonic drum configured to simulate a conga drum. The order of the tempo conditions was randomized between participants. Each person drummed along with a metronomic beat for approximately 10 s, after which they continued without the metronome for an additional 60 s. This was sufficient for the computation of a cv for each participant.

The results from this study are shown in Figure 14. At 120 bpm, the regression of log(cv) against log (height) failed to reach significance ($R^2 = .026$, $b = -0.68 \pm 0.67$, $t(39) = -1.02$, $p = .16$). The regression with log(height) at 60 bpm confirmed the existence of allometry ($R^2 = .14$, $b = -1.60 \pm 0.66$, $t(37) = -2.42$, $p = .01$), and replicated our earlier finding at this tempo.

This study goes some distance in clarifying the way temporal horizons influence the stability of drumming performances. The most important finding is that, while height does play a role in drumming precision, its influence appears to be limited to slow tempi in the vicinity of a pulse proximity constraint. At the relatively fast tempi that reflect not only peoples' spontaneous drumming preferences but also the bulk of popular music, height confers no advantage in precision. However, when people attempt to drum at slow tempi (no subdividing the interval allowed), ability, as represented through precision, does obey an allometry. This observation has been made at multiple tempi in Experiment 1 and then again at 60 bpm in Experiment 2.

This replication is important for several reasons. First and most importantly, as there is no supporting literature that contemplates allometry in temporal proximity constraints on perceptual organization, all of the findings reported in Experiment 1 have what Ioannidis (2005) refers to as "low prestudy odds." Novel reports from a single experiment must create concern that the findings will not replicate. The finding of allometry at a slow tempo in Experiment 2 is a crucial replication with new participants and a modified design. Experiment 2, however, is more than just a simple replication. The theory that we have proposed for cv allometry leads to the distinction that there will be cv allometry at 60 bpm but not at 120 bpm. Finding empirical support for this distinction is strong evidence for the theory.

Experiment 3: Allometry in the Perception of Apparent Motion

If temporal proximity constraints do indeed reflect decay lifetimes, then allometry might be quite commonplace, awaiting only the necessary psychophysics to tease it out. A second empirical demonstration of an allometry would certainly contribute to the notion that allometry is general and would also, as a matter of course, greatly enhance the "prestudy odds" of finding allometries. A good place to look for an allometry, a place where a demonstration

Figure 14
Regressions of the Coefficient of Variation Against Height in the Log–Log Plane at Two Tempi of Assessment, 60 and 120 bpm, for an Adult Sample

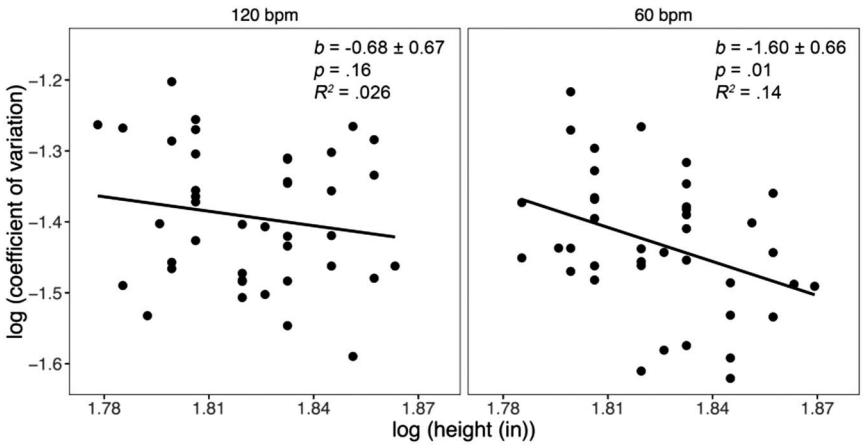

Note. The slope at 120 bpm was not statistically distinguishable from zero, while the slope at 60 bpm replicated the allometries reported in experiment 1.

would have considerable rhetorical force as a consequence of its foundational role in gestalt theory, is apparent motion.

Apparent motion is a form of temporal organization wherein two or more images that sequentially cycle on and off are perceived as a single object moving along an emergent path. The perception of a path that is not in sense data and the unification of multiple blinking images into a single persistent object has been a defining example of Gestalt since it was first discussed by Wertheimer (1912). When two images are cycled so that their presentations do not temporally overlap, the phenomenology is fairly straightforward (although, see Ekroll et al., 2008 for a full discussion of the interactions between timing variables) and involves three distinct perceptual regimes that are indexed by the stimulus onset asynchrony [SOA = image duration + inter-stimulus interval (ISI)]. At fast cycle rates (SOAs around 100 ms or less), the images tend to be perceived as flickering without a clear ordering—often referred to as simultaneity. At intermediate cycle rates (SOAs of a few hundred ms), path perception tends to be robust for image displacements measured in a few degrees of visual arc. As the SOA increases out to a half second and beyond, the path percept is replaced by the percept of succession—one image following the other with an obvious temporal ordering. The phenomenology of this second transition formally resembles that encountered in rhythmic pulse, where at sufficiently slow tempo the experience of rhythmic pulse is replaced by a succession of unrelated beats. Although the experiential qualities of rhythmic pulse and apparent motion are obviously quite different, the common role that time gaps play in organization suggests that there may be a quantity like *t-horizon* in path emergence that satisfies an allometry.

Limited measurements of temporal horizons in apparent motion have been reported using both physiological and psychophysical techniques. Wibral et al. (2009) provide an estimate for the limiting SOA in an electroencephalogram (EEG) study of apparent motion path perception. In the most simplistic terms, visual evoked potentials (VEPs) at 400 and 600 ms could be discriminated, principally at the position POz', in a specific image geometry where elements subtending 2° had a centroid separation of 4.6°. In the 400 ms condition, a signature in the sequence-sensitive difference wave appeared 90 ms after onset of the second image. This feature was largely absent at 600 ms, providing a neural correlate to self-reports of motion vividness: Strong motion at 400 ms and weak motion at 600 ms. To this extent, 600 ms might be taken as a temporal horizon for apparent motion.

A psychophysical strategy for measuring the transitional SOA was developed by Finlay and von Grünau (1987). Their method capitalized upon the fact that apparent motion is bistable near the transition SOA, alternating between path and succession percepts. The particular design employed by Finlay and von Grunau involved the self-reporting of the moment when the path percept first transitioned into succession. At a cycle rates slower than 0.75 Hz, corresponding to an SOA of 665 ms, the path percept broke down immediately independent of whether the spatial separation was 2° or 4° of visual arc. This finding is in good numerical agreement with the VEP measurements (Wibral et al., 2009) and moreover suggests that there may not be a space-time trade-off at the path/succession boundary.

Although the assessment tool developed by Finlay and von Grünau (1987) apparently does yield estimates of the critical SOA at the path/succession boundary, it is ultimately based on self-report of a perceptual state. In this early phase of investigation of allometry in apparent motion, it seemed prudent to not rely upon any form of measurement that employs self-report and to instead develop a task that permitted objective forms of measurement. In the same way that a time series provides an objective check on a person's sense of their rhythmic behavior, we required a behavioral expression that could stipulate whether or not a path was being perceived. The task we settled on was originally described in Marusich and Gilden (2014) and involved modifying a technique developed by Proffit et al. (1988) for measuring the curvature of emergent paths.

The stimulus employed by Marusich and Gilden (2014) is shown in Figure 15 below. When oriented rectangles (focusing here solely on the rectangles labeled 1 and 2) are cycled on and off, an entire class of curved paths is perceptually invited. Two members of this class are of particular theoretical import. A wand-like circular path is information minimizing; it is the simplest path, in that it involves a single rotation. There is no transformation requiring fewer operations and is an instance of Chasle's Theorem. A second path of interest is the straight line connecting the centroids of the two rectangles. This path is distance minimizing in the usual Euclidean sense, and if the path were vertical, it might describe the trajectory of a dropped object. Objective measurement of illusory path curvature was achieved simply by having the observer move a probe rectangle onto the trajectory of their perceived path. This artifice has been shown to afford precise measurement of path curvature sufficient to map out the parametric dependencies of curvature on rectangle orientation (Proffit et al., 1988).

In the following experiment, we used the probe placement method to infer path clarity as a function of SOA. The methodology is based on the expectation that the vividness or clarity of a path percept might be effectively assessed by the variance of probe placement over multiple trials. At short SOA (Proffit et al., 1988 used 250 ms), path perception is vivid, and probes may be placed with relatively low variability. As SOA increases into the regime of succession and path perception attenuates, probe placement must become more difficult and uncertain, and this uncertainty will

Figure 15
The Apparent Motion Geometry Employed in Experiment 3

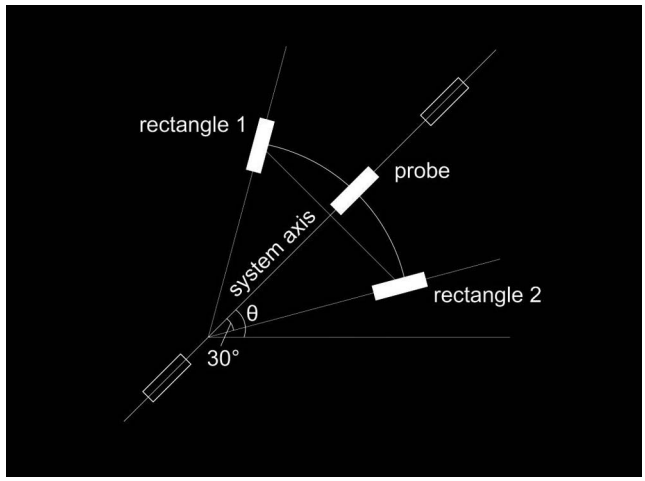

Note. Depicted are two oriented rectangles that invite a circular path percept together with a moveable probe rectangle. All elements are drawn to scale.

naturally lead to increased placement variability. In this way, we were able to construct a dependent measure that has many of the same properties as the cv. Both measures involve the placement of something into an emergent context—a probe onto an illusory path or a drum strike into a metrical context that supports pulse. Each is a measure of precision, and in both cases, precision deteriorates as the temporal distance between events approaches a proximity constraint.

These structural similarities lead to the conjecture that variability in probe placement might have the same formal structure with respect to allometry as the cv, and that the framework outlined in Figure 10 would apply to both domains. If there is an allometry in the maximum temporal gap (the critical SOA) that permits path perception, then (a) for any sufficiently slow SOA, some people will not see clear apparent motion and will contribute highly variable probe placements while others will see clearer apparent motion and will produce constrained probe placements and (b) the fractions that are in each group will scale with body size. This is exactly the analysis given to cv, and again, this framework predicts that there are temporal regimes where measures of precision are not scaling. At sufficiently short SOA where typical apparent motion studies are conducted, say, around 250 ms, most people are able to see apparent motion, and so there is no part of a residual distribution that could contribute highly variable probe placements—hence, no allometry in placement precision. The following experiment was designed to test the two main conjectures of this framework: that there are long-SOA regimes where probe placement precision follows allometric law, as well as short-SOA regimes where placement precision is height independent.

Participants

Fifty-one undergraduates at the University of Texas at Austin participated in this study. Age ranged from 18 to 25 years, and height ranged from 58.5 to 77 inches.

Stimulus and Design

The geometry of the apparent motion stimulus is shown in Figure 15. This figure is drawn to scale, and the overall dimensions reflect the computer screen area. Two rectangles, referred to here as rectangles 1 and 2, were separated by an angle in the screen plane of 60°, with their major axes aligned with a ray extending from the axis of rotation to the centroid as indicated. Proffit et al. (1988) found that rectangles oriented in this way generated the most circular wand-like apparent motion paths of all tested orientations. Along a ray bisecting the angle subtended by rectangles 1 and 2, depicted here as the system axis, we placed a movable probe rectangle aligned as shown. Movement of the probe was constrained along this ray but was otherwise free. Rectangle dimensions were 3.5 cm (3.3°) by 1.0 cm (1°), where angles here refer to degrees of visual arc subtended at a viewing distance of 60 cm. The distance between the centers of the two outer rectangles was 13 cm (12.4°), and the distance between the straight-line path and circular arc was 1.8 cm (1.7°).

Trials consisted of the three rectangles presented in succession as follows: rectangle 1—ISI—probe rectangle—ISI—rectangle 2—ISI—probe rectangle—ISI—rectangle 1, and so on. The image duration for all rectangles was 100 ms, and the ISI varied among the following values: 50, 300, 500, 700, 900, 1,100, and 1,300 ms. As the probe rectangle actively participates in the apparent motion percept, we compute the relevant SOA as that between probe and an exterior rectangle, taking on the values 150, 400, 600, 800, 1,000, 1,200, and 1,400 ms. Each SOA was tested at four different angles of the system axis (shown here as the angle θ): 45°, 135°, 225°, and 315°. Rotations of the overall display geometry were intended to prevent the enactment of placement strategies or memorization of screen positions. Trials were blocked so that the four rotations of the system were presented consecutively for a given ISI, while different ISIs were presented in a random order. At the onset of each trial, the probe rectangle was placed randomly at one of two starting positions, shown in Figure 15 as an outlined rectangle on the system axis. Starting placements at both extreme positive values (beyond the circular arc) and extreme negative values (beyond the straight-line path) discouraged the observer from enacting a stereotyped or memorized method of adjustment for placing the probe rectangle. Trials were not speeded, and participants were free to adjust the probe until they were satisfied with its placement, at which point the position was recorded with a mouse click. To be clear, none of the underlying structure in Figure 15 was visible to the participant; they only saw three blinking rectangles.

Results and Discussion

The mean and standard deviation of probe placement was computed at each SOA over the four levels of system axis orientation for each participant. The ensemble averages over participants of these statistics are shown in Figure 16. The right panel shows the mean values of probe placement, where a value of zero corresponds to a straight-line path, and a value of 107 corresponds to a circular arc. From the work of Proffit et al. (1988), whose stimulus most closely resembles ours, we expected that at short SOA (less than a few hundred milliseconds) people would place the probe on paths that were nearly but not quite circular. We take such placements as indicative of what people are perceiving. However, our study also employed large values of SOA, where probe placement was highly variable, implying attenuation of path clarity, and yet, the mean probe position did not deviate from near circularity. The implication here is either that the geometry of this stimulus invites probe placement on near circular paths, and/or people are influenced by their history of responding. Regardless, the exact same result was also obtained in Marusich and Gilden (2014) that used a similar stimulus, probe placement method, and range of SOA.

The focus of this study was not on where people place the probe but on their ability to place the probe reliably. The relevant data is shown in the left panel of Figure 16, where participant-averaged standard deviations are plotted as function of SOA. This plot possesses a number of specific features that imply that the method of probe adjustment succeeds in producing a measure of path clarity. First, at short SOA in the regime of a few hundred milliseconds, where apparent motion experiments and demonstrations are typically conducted, the probe standard deviations are both relatively constant and relatively small. The second feature is that the regime of low probe variability terminates at roughly an SOA of 600 ms that SOA which both Wibral et al. (2009) and Finlay and von Grünau (1987) have previously identified as a rough estimate of succession threshold. Beyond 600 ms, the probe variability function grows monotonically with SOA, suggesting that the task is becoming increasingly difficult as the location of the path becomes more

Figure 16

Standard Deviations and Mean Values of Probe Placement as a Function of Stimulus-Onset Asynchrony

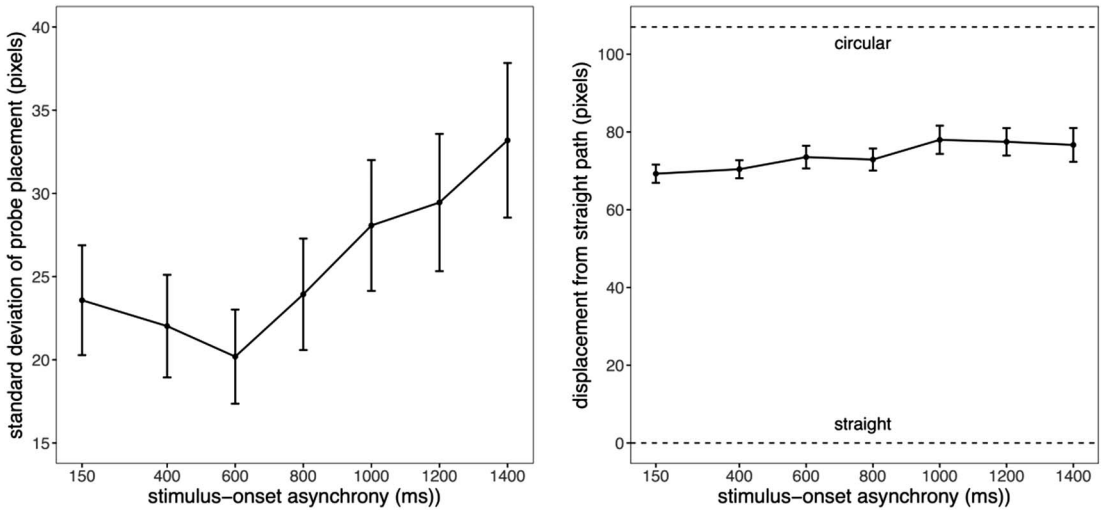

Note. Error bars depict standard error of the mean. It is evident that probe placement becomes increasing uncertain at SOA larger than 600 ms.

uncertain. Finally, at the largest SOAs, the variability is objectively large, in the sense that the full width at half maximum covers about 60 to 70 pixels in a context where 107 pixels separate the straight line from the curved path.

The development of allometric laws for probe variability closely follows the earlier work on the cv, particularly that in Experiment 2 where fast and slow tempo conditions were contrasted. What distinguishes this study is the large range of assessed SOA extending from 150 to 1,400 ms. A consequence of the extended range is that we have multiple measurements of variability in both fast blink rate (150, 400, and 600 ms) and slow blink rate (800, 1,000, and 1,200 ms) regimes. These particular groupings were motivated specifically by the appearance of the SOA function of variability as having a transition point somewhere between 600 and 800 ms. Regression analysis was then conducted on averages defined over these two groups, <150, 400, 600 ms> and <800, 1,000, 1,200 ms>, with height as the independent variable. Variability data at 1,400 ms were excluded from the slow blink rate group because it was unique in containing many outlying probe placement values—well beyond 100 pixels. The conjecture was that if probe placement behaves like drum strike placement, then the fast blink rate grouping might not show allometry, where the slow blink rate grouping would.

Figure 17 shows regressions of averaged probe placement standard deviations with participant height. The left and right panels show regressions for the low and high variability SOA groupings, respectively. As this study included only adult participants, there is no issue of intercept variation that would require an ANCOVA, and we have computed simple regression models in the log (average standard deviation)—log (height) plane to determine R^2 values and to derive power law exponents. The regression model in the slow blink rate, high variability regime has a nonzero slope, $b = -2.28 \pm 0.82$, $t(49) = -2.77$, $R^2 = .14$, $p = .004$. In contrast, the slope of the regression model in the fast blink rate, low variability regime is indistinguishable from zero. These results closely replicate the scaling of precision in rhythmic performance shown in Figure 14: Allometry at slow bpm (60 bpm) but not at fast bpm (120 bpm).

The isomorphism in precision allometries between probe placement and drum strike placement suggests that there may be an underlying allometry in the proximity constraint for apparent motion. Logically if there is an allometry in the proximity constraint for apparent motion, then the precision of probe placement should show the fast/slow distinction where precision allometry is observed. This distinction is observed, and while it does not entail the converse implication, that the proximity constraint satisfies allometry, it certainly suggests that it does. It is difficult to imagine how precision might display allometry only at slow blink rate, in the regime where path perception is attenuated, if the proximity constraint itself did not also obey an allometry.

These findings strengthen the conjecture that allometry may be a general property of perceptual organization. From a strictly probabilistic point of view, the second instance of anything makes it clear that the first instance is not isolated and that perhaps instances are common. The inference also has practical significance in that it may be methodologically more tractable to measure precision than to measure a temporal horizon. This is certainly the case with apparent motion, in that probe placement statistics do not generate any feature with SOA as an independent variable that permits the selection of an SOA horizon. To reiterate this important point, demonstrating a fast/slow distinction in the allometry of precision is a methodologically simple path to inferring allometry in the proximity constraint.

General Discussion

Scaling relationships and their associated exponents have been derived for three types of quantities: *t-horizon,* the cv in drumming performance, and the precision of probe placement in apparent motion. We have interpreted the first, *t-horizon,* as reflecting an

Figure 17

Regression Models of Probe Standard Deviations Against Height in the Log–Log Planes

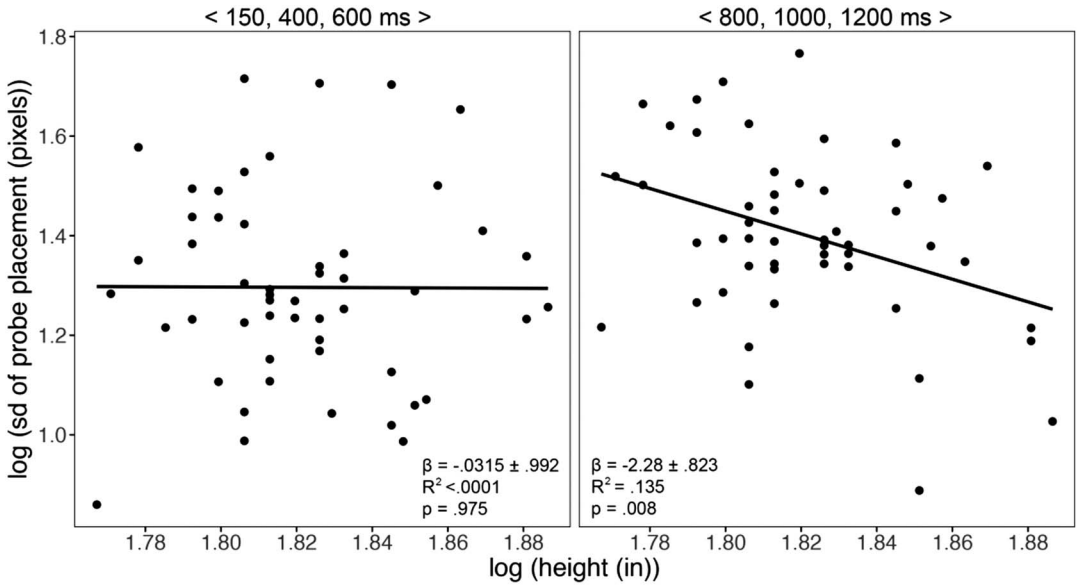

Note. Panel A shows a slope of essentially zero at short stimulus onset asynchrony (SOA; averages over 150, 400, and 600 ms). Panel B shows a statistically resolved negative slope at longer SOA (averages over 800, 1000, and 1200 ms).

activation lifetime, τ. Under this interpretation, *t-horizon* is a characteristic timescale of a memory process—it is a memory property. Measures of precision, coefficients of variation, and standard deviations are not properties but behavioral outcomes—outcomes theorized to inherit their scaling from the scaling of an underlying proximity constraint. This distinction informs the kind of interpretation that we bring to the allometric laws that have been derived. Of the three scaling quantities that have been produced, only the exponent of *t-horizon* permits a theoretical account. The exponents of precision allometries will be interpreted in terms of the residuals of proximity regressions.

Interpreting the *t-horizon* Proximity Constraint Exponent

Within the framework that has been developed to understand the prevalence of 2 ± 1 s as a proximity constraint (Figure 1), proximity constraints as a class were conceptualized as reflecting activation lifetimes. What factors might be relevant to an allometry in an activation decay lifetime are, however, not clear given that proximity constraints play such an important role in determining group memberships. So although an activation lifetime might be conceptualized in terms of brain function, what proximity constraints do, their purpose, must be conceptualized in ecological terms, as scene formation is what makes the world a meaningful place. This blending of system levels suggests that much more must be understood about embodiment before a theory of proximity constraint scaling is approachable. In the absence of a theory of *t-horizon* allometry, it is nevertheless worthwhile to place its exponent into the broader context of physiological and behavioral allometries. To this end, we examine the allometry for rhythmic pulse in terms of the allometries produced by the two most important forms of human energy expenditure; locomotion and basal metabolism.

Scaling of Energetically Efficient Body Motion

The most common form of rhythmic motion is walking, and to the extent that the experience of rhythm involves the motion of jointed limbs, an analysis of walking energetics provides a good starting point for deriving an allometry relevant to rhythmic expression. The kinematics of walking is a topic of some complexity that has been approached both through empirical measurement (Burdett et al., 1983; Rose et al., 1991), and through the construction of formal models (Anderson & Pandy, 2001; Kuo, 2001, 2002). There is, however, one elementary property of walking that immediately leads to a scaling law. Recognizing that it is possible for walking to be conducted at a range of speeds, the energy output per meter walked (a definition of efficiency) is minimized at a unique speed (Rose et al., 1994). The existence of an energy expenditure minimum in locomotion is specific to walking kinematics and is a consequence of the fact that walking is basically a driven pendular motion; legs in walking motion effectively function as compound pendula anchored at the waist. Pendula display the property of resonance, such that their response amplitude is maximal when a periodic driving force is matched in frequency to the natural period. The consequence of this resonance for animal locomotion is that energy consumption is minimized when the gait period matches the natural pendular period. The natural pendular period scales as the square root of leg length, and this square root relation governs all of the relevant timescales for motion at the energy consumption minimum. The crossing time, the time for a person to traverse the extent of their own body, is a timescale of obvious ecological consequence, and it will scale with the square root of height.

The notion that gait period might be a factor accounting for individual differences in specific perceptual tasks is not novel, particularly in relation to tasks involving rhythmic pulse, an experience that is typically expressed through body motion. Todd et al. (2007), for example, invoked individual differences in gait period to explain their finding that body size was related to the transitional tempo at which perceptually ambiguous meters were resolved in a classification task. This same perspective was reiterated by Dahl et al. (2014) in a study showing that preferred dance tempo is correlated with body size. It is noteworthy that Todd et al. did not explicitly derive the pendular period exponent from an allometric regression model. Rather, the relevance of pendula to perceived meter arose as part of a hypothesis—that a perceptual task involving rhythm might be informed by physical properties of the way human bodies are constructed and move.

Metabolic Scaling

The physical processes associated with thermogenesis and radiative heat loss create a specific allometric exponent for key time intervals associated with life—heart-beat period, respiration period, blood circulation period, and animal lifetime. Across mammals, the $M^{3/4}$ version of the Kleiber Law for total energy production leads to a $M^{1/4}$ scaling law for this class of periods. This exponent, however, may not hold for human populations (or for any particular species), and as *t-horizon* applies to humans, here we will derive a metabolic allometric law that is specific to humans.

There are two approaches to the derivation of the relevant exponent. One avenue is through regression analysis of human metabolic data. The appropriate statistical description has been developed by Johnstone et al. (2005) who constructed a Kleiber-type law for human adults. Based upon a sample of 150 adults (ages 21 to 64 years), a multiple regression model of log (basal metabolic rate—BMR) was formed that included log(fat free mass—FFM), log (fat mass—FM), and age as regressors. This three-factor model accounted for 71% of the variance in log(BMR), most of this due to one factor—FFM. log(FFM) accounted for 63% of the variance with a slope of 0.62, while log(FM) and age accounted for only 6.7% and 1.7%, respectively. So, to a fair approximation, BMR in human adults is determined by FFM and scales almost isometrically with it (0.66 is nominal surface area geometric scaling). Metabolic timescales (heart beat period, respiration period, blood circulation time) are derived as the reciprocal of the mass specific BMR, implying that temporal attributes of human metabolism scale roughly as $\mathrm{FFM}^{.38}$. To put metabolic timescales onto a footing that can be used for comparison with *t-horizon*, we desire a relation that is based just on stature. It has been known since Quetelet (1842) that weight in adults' scales as height squared. This measurement was refined by Heymsfield et al. (2007), in breaking out the separate contributions of FFM and FM. FFM was found to have a power law relationship with height with exponents of 1.86 and 2.05 in men and women, respectively—sufficiently close to two for our purposes. From these power laws, we deduce that metabolic timescales roughly satisfy a $\mathrm{height}^{.76}$ law in human adults.

A second and perhaps more straightforward route to the allometric scaling of heart beat period would be to simply access the height and resting pulse data that are collected routinely by health professionals. It appears, however, that such data are rarely amassed for the purposes of regression analysis. One study that did perform this analysis was conducted by Smulyan et al. (1998), and their simple regression of heart period on height (their Figure 2) permitted us to determine an empirical power law for heart period in terms of height. From their data, the inferred relation is heart period $\sim$ $\mathrm{height}^{.79}$, which is in close agreement with the exponent derived from FFM scaling.

The measurement of *t-horizon* in adults produced four distinct estimates of height exponent: 0.64 ± 0.24 in a first round time series visual analysis, 0.81 ± 0.24 in a second round time visual series analysis that also benefited from lag-1 autocorrelations and coefficients of variation, 0.72 ± 0.27 from Madison's diffusion rate statistic, and finally 0.82 ± 0.16, produced on the basis of second round estimates in an ANCOVA with children. Taking these exponents and associated errors at face value, it does appear that *t-horizon* and metabolic timescales obey similar scaling relations with body size. If the ANCOVA model is taken as a best estimate for the *t-horizon* scaling exponent, the square root law for locomotion is more than two standard deviations removed, while there is obvious close agreement with heart period scaling in humans.

This finding, although not explaining the *t-horizon* exponent, is nevertheless theoretically important and demonstrates how this approach goes beyond simple correlational analysis. First, disassociating *t-horizon* from locomotion is interesting in itself. In the early stages of this investigation we wondered whether the gait cycle might literally create temporal proximity constraints. From a perhaps naive ecological point of view, every step we take does take us to a new point of observation and so potentially to a new scene. Again, naively, it does seem reasonable that the time to complete a gait cycle might then serve as proximity constraint for scene formation. And, it is the case that the pendular period that sets the gait cycle period is close to 2 ± 1 s, and so is numerically in agreement with observed proximity constraints. This story, however compelling, turns out to be improbable if the standard error of the estimate of the *t-horizon* exponent is credible. The positive result, that *t-horizon* has heart period scaling, appears to be coincidental, but it is nevertheless interesting in view of the circumstance that both are related to cooling. Heart period becomes related to cooling by virtue of its scaling exponent being set by the balancing of thermogenesis with radiative losses at the body's surface (Johnstone et al., 2005). *t-horizon* is related to cooling by virtue of what it is; it is conceptualized here as being a measurement of τ, which is by its nature a cooling timescale. In essence, our work on *t-horizon* can be summarized by the idea that the shedding of memory activation has the isometric scaling of body cooling.

Perspective on the Exponents Derived for Measures of Precision

Measurement of precision in drumming and probe positioning also led to scaling laws with body size, but the derived allometric exponents do not invite an analysis framed in terms of physical properties. Precision is a behavioral outcome, and within the framework we have developed, its scaling is inherited from the underlaying scaling of a proximity constraint such that the associated exponents are unlikely to be susceptible to biological or physical explanation. Specifically, the theoretical outline shown in Figure 10 clarifies that there are three independent contributions to a precision exponent: the exponent of the proximity constraint, the width of the residual distributions, and the jump in variability

between the regime of temporal integration and the regime of succession. Of these three factors, only the scaling properties of the proximity constraint may be amenable to a biological or psychological explanation.

The widths of the residual distributions play a key role in the way precision acquires allometry. That residuals play a role in setting precision exponents is problematic, in so far as residuals represent variability unexplained by allometry. In this sense, residuals are outside of the scope of allometry, even if they are explained by other aspects of physics or biology. In fact, the residuals may have interesting but unknown properties that have nothing to do with the body. For example, in previous work, we showed that the much of the unexplained variance in reaction time residuals may be explained as 1/*f* noise (Gilden, 2001), a type of fluctuation of significance in physical theory (Press, 1978), but which is entirely unrelated to the experimental designs that generated the residuals in the first place. Similarly, theories of allometry may have nothing to say about the residual variation that enters into the production of precision exponents.

The final factor, the discontinuity in variability across the proximity constraint, is based on a number of factors that are by their nature ill defined. The principal problem is that only on the temporal integration side of the proximity constraint is variability likely to be linked to a lawful process. Variability in regimes of temporal integration presumably reflects lawful properties of a perceptually organized state. This is at root the reason that it is meaningful to inquire, for example, into whether rhythmic behavior exhibits the Weberian property—the property of perceptual systems that just-noticeable differences are proportional to the magnitude of ambient stimulation. On the succession side of the proximity constraint, the situation is substantially different for the single reason that behavioral variability does not reflect upon a perceived quantity. In drumming performance, for example, variability in the regime of succession involves attempts to place drum strikes in time in the absence of a sense of beat relatedness and where pulse is not emerging. Probe placement variability in the succession regime of apparent motion arises from attempting to place a probe onto a path that has not emerged. Succession is generally the experience of temporal distribution when perceptual integration has failed, and any response that in fact requires integration can only reflect the strategies of a person struggling toward a meaningful response. These strategies may not lead to well-defined and quantifiable behavior. As an example, random walking in the time series of interbeat intervals is observed when rhythmic pulse is lost during a drumming performance. As random walks exemplify an inherently nonstationary process, cv values that are based upon random walks are also nonstationary and so are not fixed properties of any system. In the context of probe placement onto an illusory path in the succession regime, precision depends critically on how people respond to the requirement that a probe be placed onto a path that is not perceived. In this case, probe positions can only reflect the sense, demand characteristic actually, that the choices be proximal to the inducing rectangles and not, say, at the screen's edge. The implication then is that contrasts in precision across a proximity constraint may not be meaningful or interpretable. As these contrasts factor into the derived value of the slopes in an allometric regression, the slopes (exponents) are also difficult to interpret. The conclusion here is that nonzero exponents in precision allometry have methodological utility, in that they imply the existence of allometry in a proximity constraint, but caution must be taken in interpreting the exponent magnitudes.

Concluding Remarks

In this article, we propose the theory that temporal proximity constraints arise from an autonomous memory process of activation decay. In this theory, proximity constraints reflect decay lifetimes, and this identification led to the conjecture that proximity constraints as a class might obey allometric laws. This conjecture departs in several ways from asking whether a particular percept, judgment, or behavior is correlated with body size. First, the class of proximity constraints is unbounded and includes all instances of temporal integration where organized states dissolve into succession as the event arrival rate decreases. In essence, the conjecture concerns the myriad processes that fuse the flux of temporal experience into meaningful scenes. Second, producing an allometry is not quite the same thing as producing a correlation. Allometry is a form of measurement, and while it necessarily involves a correlational analysis, the focus of allometry is on the production of a power-law exponent. In physical and biological contexts, the exponents are of fundamental importance in theory building. Allometry has not heretofore been an issue in psychological science, and it remains to be seen what role allometric exponents will play in theory construction.

A conjecture about the class of proximity constraints cannot be tested in its entirety, but evidence was presented that allometric laws exist for the proximity constraints limiting the formation of rhythmic pulse and the perception of illusory apparent motion paths. The quality of data inherent in the time series produced by a drumming performance allowed a more or less direct measurement of the power-law exponent governing rhythmic pulse. This exponent had a magnitude that was remarkably close to the exponents for timescales associated with basal metabolism. Further work may clarify if proximity constraints for other forms of grouping have similar scaling.

In the context of apparent motion, our method was ill suited to measuring a proximity constraint, but it was able to produce a measure of precision in probe placement that turned out to have exactly the same allometric properties as the cv in drumming performance. Such a convergence between two very different experiences suggests that placing a drum strike into a metrical context and placing a probe onto an apparent motion path are tapping into a common process. That process, in the framework we have developed, is that of activation decay.

This work clearly opens up other avenues of investigation. Any methodology that produces a behavioral variable indexed to the strength of temporal integration may be able to produce an allometry, if one exists. There may also be further generalizations beyond proximity constraints. In fact, any behavior that involves the discrimination of temporal intervals may be in play, in so far as judgments that involve the sense of time passage may be utilizing mechanisms of activation decay.

References

Allan, L. G. (1979). The perception of time. *Perception & Psychophysics*, *26*(5), 340–354. https://doi.org/10.3758/BF03204158

Anderson, F. C., & Pandy, M. G. (2001). Dynamic optimization of human walking. *Journal of Biomechanical Engineering*, *123*(5), 381–390. https://doi.org/10.1115/1.1392310

Aschersleben, G. (2002). Temporal control of movements in sensorimotor synchronization. *Brain and Cognition*, *48*(1), 66–79. https://doi.org/10.1006/brcg.2001.1304

Bååth, R. (2015). Subjective rhythmization: A replication and an assessment of two theoretical explanations. *Music Perception*, *33*(2), 244–254. https://doi.org/10.1525/mp.2015.33.2.244

Burdett, R. G., Skrinar, G. S., & Simon, S. R. (1983). Comparison of mechanical work and metabolic energy consumption during normal gait. *Journal of Orthopaedic Research*, *1*(1), 63–72. https://doi.org/10.1002/jor.1100010109

Catania, A. C. (1970). Reinforcement schedules and psychophysical judgment. In W. N. Schoenfeld (Ed.), *Theory of reinforcement schedules* (pp. 1–42). Appleton-Century-Crofts.

Dahl, S., Huron, D., Brod, G., & Altenmüller, E. (2014). Preferred dance tempo: Does sex or body morphology influence how we groove? *Journal of New Music Research*, *43*(2), 214–223. https://doi.org/10.1080/09298215.2014.884144

Drake, C., Jones, M. R., & Baruch, C. (2000). The development of rhythmic attending in auditory sequences: Attunement, referent period, focal attending. *Cognition*, *77*(3), 251–288. https://doi.org/10.1016/S0010-0277(00)00106-2

Eck, D. (2006). Identifying temporal and metrical structure with an autocorrelation phase matrix. *Music Perception*, *24*(2), 167–176. https://doi.org/10.1525/mp.2006.24.2.167

Ekroll, V., Faul, F., & Golz, J. (2008). Classification of apparent motion percepts based on temporal factors. *Journal of Vision*, *8*(4), Article 31. 1–22. https://doi.org/10.1167/8.4.31

Engström, D. A., Kelso, J. A. S., & Holroyd, T. (1996). Reaction-anticipation transitions in human perception-action patterns. *Human Movement Science*, *15*(6), 809–832. https://doi.org/10.1016/S0167-9457(96)00031-0

Etani, T., Marui, A., Kawase, S., & Keller, P. E. (2018). Optimal tempo for groove: Its relation to directions of body movement and Japanese nori. *Frontiers in Psychology*, *9*, Article 462. https://doi.org/10.3389/fpsyg.2018.00462

Finlay, D., & von Grünau, M. (1987). Some experiments on the breakdown effect in apparent motion. *Perception & Psychophysics*, *42*(6), 526–534. https://doi.org/10.3758/BF03207984

Fraisse, P. (1984). Perception and estimation of time. *Annual Review of Psychology*, *35*(1), 1–36. https://doi.org/10.1146/annurev.ps.35.020184.000245

Friberg, A., & Sundberg, J. (1995). Time discrimination in a monotonic, isochronous sequence. *The Journal of the Acoustical Society of America*, *98*(5), 2524–2531. https://doi.org/10.1121/1.413218

Gilden, D. L. (1997). Fluctuations in the time required for elementary decisions. *Psychological Science*, *8*(4), 296–301. https://doi.org/10.1111/j.1467-9280.1997.tb00441.x

Gilden, D. L. (2001). Cognitive emissions of 1/f noise. *Psychological Review*, *108*(1), 33–56. https://doi.org/10.1037/0033-295X.108.1.33

Gilden, D. L. (2009). Global model analysis of cognitive variability. *Cognitive Science*, *33*(8), 1441–1467. https://doi.org/10.1111/j.1551-6709.2009.01060.x

Gilden, D. L., & Marusich, L. R. (2009). Contraction of time in attention-deficit hyperactivity disorder. *Neuropsychology*, *23*(2), 265–269. https://doi.org/10.1037/a0014553

Gilden, D. L., Thornton, T., & Mallon, M. W. (1995). 1/f noise in human cognition. *Science*, *267*(5205), 1837–1839. https://doi.org/10.1126/science.7892611

Grondin, S. (2010). Timing and time perception: A review of recent behavioral and neuroscience findings and theoretical directions. *Attention, Perception & Psychophysics*, *72*(3), 561–582. https://doi.org/10.3758/APP.72.3.561

Grondin, S., Meilleur-Wells, G., & Lachance, R. (1999). When to start explicit counting in a time-intervals discrimination task: A critical point in the timing process of humans. *Journal of Experimental Psychology: Human Perception and Performance*, *25*(4), 993–1004. https://doi.org/10.1037/0096-1523.25.4.993

Heusner, A. A. (1982). Energy metabolism and body size. I. Is the 0.75 mass exponent of Kleiber's equation a statistical artifact? *Respiration Physiology*, *48*(1), 1–12. https://doi.org/10.1016/0034-5687(82)90046-9

Heymsfield, S. B., Gallagher, D., Mayer, L., Beetsch, J., & Pietrobelli, A. (2007). Scaling of human body composition to stature: New insights into body mass index. *The American Journal of Clinical Nutrition*, *86*(1), 82–91. https://doi.org/10.1093/ajcn/86.1.82

Ioannidis, J. P. (2005). Why most published research findings are false. *PLOS Medicine*, *2*(8), Article e124. https://doi.org/10.1371/journal.pmed.0020124

Johnstone, A. M., Murison, S. D., Duncan, J. S., Rance, K. A., & Speakman, J. R. (2005). Factors influencing variation in basal metabolic rate include fat-free mass, fat mass, age, and circulating thyroxine but not sex, circulating leptin, or triiodothyronine. *The American Journal of Clinical Nutrition*, *82*(5), 941–948. https://doi.org/10.1093/ajcn/82.5.941

Kuo, A. D. (2001). A simple model of bipedal walking predicts the preferred speed-step length relationship. *Journal of Biomechanical Engineering*, *123*(3), 264–269. https://doi.org/10.1115/1.1372322

Kuo, A. D. (2002). Energetics of actively powered locomotion using the simplest walking model. *Journal of Biomechanical Engineering*, *124*(1), 113–120. https://doi.org/10.1115/1.1427703

Large, E. W. (2000). On synchronizing movements to music. *Human Movement Science*, *19*(4), 527–566. https://doi.org/10.1016/S0167-9457(00)00026-9

Large, E. W., & Jones, M. R. (1999). The dynamics of attending: How people track time-varying events. *Psychological Review*, *106*(1), 119–159. https://doi.org/10.1037/0033-295X.106.1.119

Large, E. W., & Kolen, J. F. (1994). Resonance and the perception of musical meter. *Connection Science*, *6*(2–3), 177–208. https://doi.org/10.1080/09540099408915723

Large, E. W., & Palmer, C. (2002). Perceiving temporal regularity in music. *Cognitive Science*, *26*(1), 1–37. https://doi.org/10.1207/s15516709cog2601_1

Large, E. W., & Snyder, J. S. (2009). Pulse and meter as neural resonance. *Annals of the New York Academy of Sciences*, *1169*(1), 46–57. https://doi.org/10.1111/j.1749-6632.2009.04550.x

Li, X., Wang, X., Zhang, J., & Wu, L. (2015). Allometric scaling, size distribution and pattern formation of natural cities. *Palgrave Communications*, *1*(1), 1–11. https://doi.org/10.1057/palcomms.2015.17

Lindstedt, S. L., & Calder, W. A. (1981). Body size, physiological time, and longevity of homeothermic animals. *The Quarterly Review of Biology*, *56*(1), 1–16. https://doi.org/10.1086/412080

Macefield, G., Gandevia, S. C., & Burke, D. (1989). Conduction velocities of muscle and cutaneous afferents in the upper and lower limbs of human subjects. *Brain: A Journal of Neurology*, *112*(6), 1519–1532. https://doi.org/10.1093/brain/112.6.1519

Madison, G. (2001). Variability in isochronous tapping: Higher order dependencies as a function of intertap interval. *Journal of Experimental Psychology: Human Perception and Performance*, *27*(2), 411–422. https://doi.org/10.1037/0096-1523.27.2.411

Marusich, L. R., & Gilden, D. L. (2014). Assessing temporal integration spans in ADHD through apparent motion. *Neuropsychology*, *28*(4), 585–593. https://doi.org/10.1037/neu0000080

Mates, J., Müller, U., Radil, T., & Pöppel, E. (1994). Temporal integration in sensorimotor synchronization. *Journal of Cognitive Neuroscience*, *6*(4), 332–340. https://doi.org/10.1162/jocn.1994.6.4.332

Matsuda, S., Matsumoto, H., Furubayashi, T., Hanajima, R., Tsuji, S., Ugawa, Y., & Terao, Y. (2015). The 3-second rule in hereditary pure cerebellar ataxia: A synchronized tapping study. *PLOS ONE*, *10*(2), Article e0118592. https://doi.org/10.1371/journal.pone.0118592

McAuley, J. D., Jones, M. R., Holub, S., Johnston, H. M., & Miller, N. S. (2006). The time of our lives: Life span development of timing and event tracking. *Journal of Experimental Psychology: General*, *135*(3), 348–367. https://doi.org/10.1037/0096-3445.135.3.348

Meyer, D. E., & Schvaneveldt, R. W. (1971). Facilitation in recognizing pairs of words: Evidence of a dependence between retrieval operations. *Journal of Experimental Psychology*, *90*(2), 227–234. https://doi.org/10.1037/h0031564

Müller, K., Aschersleben, G., Schmitz, F., Schnitzler, A., Freund, H. J., & Prinz, W. (2008). Inter- versus intramodal integration in sensorimotor synchronization: A combined behavioral and magnetoencephalographic study. *Experimental Brain Research*, *185*(2), 309–318. https://doi.org/10.1007/s00221-007-1155-1

Navarro, D. J., Pitt, M. A., & Myung, I. J. (2004). Assessing the distinguishability of models and the informativeness of data. *Cognitive Psychology*, *49*(1), 47–84. https://doi.org/10.1016/j.cogpsych.2003.11.001

Niklas, K. J. (1994). *Plant allometry: The scaling of form and process*. University of Chicago Press.

Pélabon, C., Bolstad, G. H., Egset, C. K., Cheverud, J. M., Pavlicev, M., & Rosenqvist, G. (2013). On the relationship between ontogenetic and static allometry. *American Naturalist*, *181*(2), 195–212. https://doi.org/10.1086/668820

Perin, C. T. (1943). A quantitative investigation of the delay-of-reinforcement gradient. *Journal of Experimental Psychology*, *32*(1), 37–51. https://doi.org/10.1037/h0056738

Pöppel, E. (1997). A hierarchical model of temporal perception. *Trends in Cognitive Sciences*, *1*(2), 56–61. https://doi.org/10.1016/S1364-6613(97)01008-5

Pöppel, E. (2009). Pre-semantically defined temporal windows for cognitive processing. *Philosophical Transactions of the Royal Society of London. Series B, Biological Sciences*, *364*(1525), 1887–1896. https://doi.org/10.1098/rstb.2009.0015

Press, W. H. (1978). Flicker noises in astronomy and elsewhere. *Comments on Astrophysics*, *7*(4), 103–119. https://adsabs.harvard.edu/full/1978ComAp...7..103P

Proffit, D. R., Gilden, D. L., Kaiser, M. K., & Whelan, S. M. (1988). The effect of configural orientation on perceived trajectory in apparent motion. *Perception & Psychophysics*, *43*(5), 465–474. https://doi.org/10.3758/BF03207882

Quetelet, A. (1842). *A treatise on man and the development of his faculties: Now first translated into English*. William and Robert Chambers.

Quinlan, P. T., & Wilton, R. N. (1998). Grouping by proximity or similarity? Competition between the Gestalt principles in vision. *Perception*, *27*(4), 417–430. https://doi.org/10.1068/p270417

Richman, J. S., & Moorman, J. R. (2000). Physiological time-series analysis using approximate entropy and sample entropy. *American Journal of Physiology. Heart and Circulatory Physiology*, *278*(6), H2039–H2049. https://doi.org/10.1152/ajpheart.2000.278.6.H2039

Roberts, S. (1981). Isolation of an internal clock. *Journal of Experimental Psychology: Animal Behavior Processes*, *7*(3), 242–268. https://doi.org/10.1037/0097-7403.7.3.242

Roberts, S., & Church, R. M. (1978). Control of an internal clock. *Journal of Experimental Psychology: Animal Behavior Processes*, *4*(4), 318–337. https://doi.org/10.1037/0097-7403.4.4.318

Roberts, W. A. (1998). Timing. In *Principles of animal cognition* (pp. 241–265). McGraw-Hill.

Roediger, H. L., & McDermott, K. B. (1995). Creating false memories: Remembering words not presented in lists. *Journal of Experimental Psychology: Learning, Memory, and Cognition*, *21*(4), 803–814. https://doi.org/10.1037/0278-7393.21.4.803

Rose, J., Gamble, J. G., Lee, J., Lee, R., & Haskell, W. L. (1991). The energy expenditure index: A method to quantitate and compare walking energy expenditure for children and adolescents. *Journal of Pediatric Orthopedics*, *11*(5), 571–578. https://doi.org/10.1097/01241398-199109000-00002

Rose, J., Ralston, H., & Gamble, J. (1994). Energetics of walking. In J. Rose & J. Gamble (Eds.), *Human walking* (2nd ed., pp. 45–72). Williams & Wilkins.

Scheirer, E. D. (1998). Tempo and beat analysis of acoustic musical signals. *The Journal of the Acoustical Society of America*, *103*(1), 588–601. https://doi.org/10.1121/1.421129

Simon, H. A. (1966). A note on Jost's Law and exponential forgetting. *Psychometrika*, *31*(4), 505–506. https://doi.org/10.1007/BF02289520

Smulyan, H., Marchais, S. J., Pannier, B., Guerin, A. P., Safar, M. E., & London, G. M. (1998). Influence of body height on pulsatile arterial hemodynamic data. *Journal of the American College of Cardiology*, *31*(5), 1103–1109. https://doi.org/10.1016/S0735-1097(98)00056-4

Steinman, R. M., Pizlo, Z., & Pizlo, F. J. (2000). Phi is not beta, and why Wertheimer's discovery launched the Gestalt revolution. *Vision Research*, *40*(17), 2257–2264. https://doi.org/10.1016/S0042-6989(00)00086-9

Thomas, P. K., Sears, T. A., & Gilliatt, R. W. (1959). The range of conduction velocity in normal motor nerve fibers to the small muscles of the hand and foot. *Journal of Neurology, Neurosurgery, and Psychiatry*, *22*(3), 175–181. https://doi.org/10.1136/jnnp.22.3.175

Thut, G., Schyns, P. G., & Gross, J. (2011). Entrainment of perceptually relevant brain oscillations by non-invasive rhythmic stimulation of the human brain. *Frontiers in Psychology*, *2*, Article 170. https://doi.org/10.3389/fpsyg.2011.00170

Todd, N. P. M., Cousins, R., & Lee, C. S. (2007). The contribution of anthropometric factors to individual differences in the perception of rhythm. *Empirical Musicology Review*, *2*(1), 1–13. https://doi.org/10.18061/1811/24478

Warren, R. M., Gardner, D. A., Brubaker, B. S., & Bashford, J. A., Jr. (1991). Melodic and nonmelodic sequences of tones: Effects of duration on perception. *Music Perception*, *8*(3), 277–289. https://doi.org/10.2307/40285503

Wearden, J. H. (1991). Do humans possess an internal clock with scalar timing properties? *Learning and Motivation*, *22*(1–2), 59–83. https://doi.org/10.1016/0023-9690(91)90017-3

Wertheimer, M. (1912). Experimentelle studien uber das sehen von bewegung. *Zeitschrift für Psychologie mit Zeitschrift für Angewandte Psychologie*, *61*, 161–265.

West, G. B., & Brown, J. H. (2005). The origin of allometric scaling laws in biology from genomes to ecosystems: Towards a quantitative unifying theory of biological structure and organization. *The Journal of Experimental Biology*, *208*(9), 1575–1592. https://doi.org/10.1242/jeb.01589

White, P. A. (2017). The three-second "subjective present": A critical review and a new proposal. *Psychological Bulletin*, *143*(7), 735–756. https://doi.org/10.1037/bul0000104

Wibral, M., Bledowski, C., Kohler, A., Singer, W., & Muckli, L. (2009). The timing of feedback to early visual cortex in the perception of long-range apparent motion. *Cerebral Cortex*, *19*(7), 1567–1582. https://doi.org/10.1093/cercor/bhn192

Wing, A. M., & Kristofferson, A. B. (1973). Response delays and the timing of discrete motor responses. *Attention, Perception & Psychophysics*, *14*(1), 5–12. https://doi.org/10.3758/BF03198607

Wixted, J. T. (2004). On common ground: Jost's (1897) law of forgetting and Ribot's (1881) law of retrograde amnesia. *Psychological Review*, *111*(4), 864–879. https://doi.org/10.1037/0033-295X.111.4.864

(*Appendix follows*)

Appendix

The first issue to be addressed in a study of proximity constraint scaling is how the constraint might be measured. In the context of rhythmic pulse, the measurement of a proximity constraint comes down to finding the slowest limiting tempo at which a person is able to perform a rhythmically stable performance. The interbeat interval corresponding to this tempo serves as a measurement of the maximal time interval, *t-horizon*, over which successive beats can be temporally fused to support the emergence of pulse. The technique that is used for assessing *t-horizon* is of fundamental importance in this context, as the quality of the assessment tool directly impacts the degree to which variation may be reliably attributed to underlying scaling structure. This is not a form of measurement that involves rote computation as might be involved in ANOVA and the assessment of statistical significance. Some degree of invention is required. As this study is not the first to attempt measurement of *t-horizon,* it is worthwhile to review and evaluate previous efforts. To appreciate what is involved in assessing *t-horizon,* it will help to review what drumming data look like at various tempi.

Elementary Rhythm Phenomenology

Figure A1 (reprinted from Gilden and Marusich, 2009) plots the time series of interbeat intervals for one participant, drumming (on a real drum with midi output) at a variety of tempi in a continuation paradigm. In the continuation method, the participant drums or taps along with an auditory click track for a preset number of beats or period of time, after which the participant's task is to continue drumming or tapping at the preassigned tempo. The time series of interbeat intervals is formed by computing the time intervals between temporally adjacent drum strikes and is the raw form of drumming data. A simple visual inspection suffices to make most of the relevant points about what drumming data might display at various tempi in a continuation paradigm.

The first observation to be made is that this person is on occasion able to drum in a regular and stable fashion. At tempi $\geq$ 40 bpm, the respective time series of interbeat intervals appear to be statistically stationary in the sense that the mean and standard deviation are fairly constant over the duration of the performance. That the amplitude of fluctuation increases monotonically with decreasing tempo, σ (120 bpm) $< \sigma$ (60 bpm) $< \sigma$ (40 bpm), may be largely explained in terms of the Weberian property that timing errors increase in magnitude in proportion to the magnitude of the interval being expressed. That is, the fluctuations in Figure A1 would be expected to be some three times larger at 40 bpm than they are at 120 bpm. The Weberian property is well documented for rhythmic tapping in continuation paradigms (see McAuley et al., 2006 and Madison, 2001), as well as in time interval discrimination more generally (Friberg & Sundberg, 1995). The second observation is that performances slower than 40 bpm are manifestly not stationary but rather wander in tempo. These visual distinctions are striking, and it is this kind of discriminating evidence that gives the continuation method its power. We interpret the two regimes of performance as indicating the presence and absence of the feeling of rhythmic pulse, a conclusion that cannot be formally proven but which will be defended throughout, as we review the various ways rhythm has been investigated.

To fully understand what the time series at the two slowest tempi in Figure A1 are illustrating, it is useful to contemplate what the participant might be experiencing. The task confronting a performer when asked to drum even when lost is admittedly difficult, but it must be encountered in any study that attempts to measure proximity constraints in beat organization. It is especially difficult in a continuation paradigm where there is no click track that can corral the performer back onto the beat. In real performance situations, the general rule when one has lost rhythmic pulse is to stop and listen to the other performers, and then to resume when the measure structure has been reacquired and the "one" beat has been located. Here, there are no measures, no other performers, and the drummer must suffer through whatever they can manage to produce for the period of time they have been allocated. Consider then the options available to a performer who is attempting to strike a drum at regular intervals in a duple meter at a tempo that is so slow that they are unable develop an adequate sense of rhythmic pulse. One option is to attempt to subdivide the target interval by counting out loud or subvocally. This strategy must be either prohibited through instruction (Madison, 2001) or through tying up the vocalization apparatus through a secondary task (Gilden & Marusich, 2009). Other strategies for subdivision that involve movement of limbs or head must also be prohibited, and in practice, it is essential for an experimenter to be

Figure A1
Time Series of Interbeat Intervals for Nonsynchronized Drumming at Target Tempi of 15, 30, 40, 60, and 120 bpm (Target Time Intervals of 4, 2, 1.5, 1, and 0.5 s, Respectively), Reprinted From Gilden and Marusich (2009)

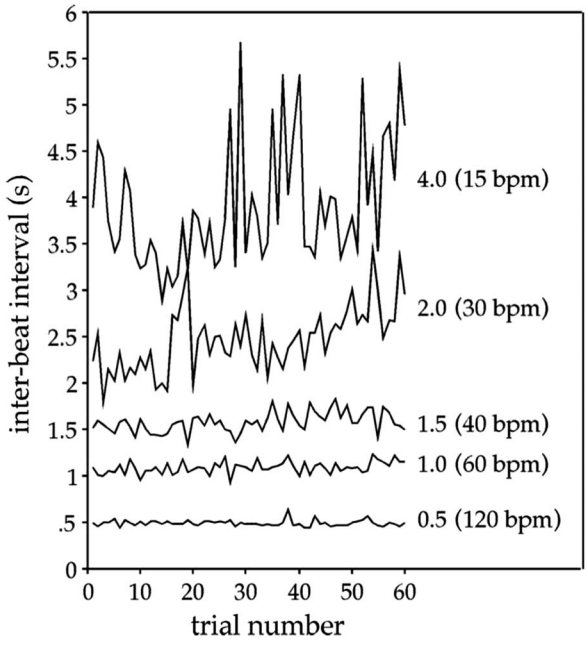

Note. Trial number here refers to the ordering of successive drum strikes. The *i*th trial number defines the interbeat interval between the *i*th and $(i - 1)$ st drum strike. Loss of rhythm is evidenced by wandering in the time series at tempi slower than 40 bpm.

(*Appendix continues*)

present in all phases of data collection. The only permissible recourse available to a lost performer is to strike the drum when they think an appropriate amount of time has elapsed. The performer, in this instance, does not know the true appropriate amount of time, in that they have lost rhythmic pulse and so have no sense of pattern into which they might place the next drum strike. One interval of time that may be available, and which could serve as an appropriate interval, is their recollection of the previous interval, the interbeat interval terminated by their last drum strike. In this circumstance, the performer effectively enacts a recursive relation; the current interval is executed as the memory of the last interval. This recursive relation may be expressed by a simple generating function for a random walk, $X(t + 1) = X(t) +$ Random deviate, or by some more elaborate version of autoregression. For the purposes here, it suffices to note that attempts to replicate the previous interval will invariably generate a contour depicting diffusion. The performance at 30 bpm in Figure A1 is typical of a performance that slowly diffuses in tempo. At extremely slow tempi, even the last interval may not be memorially available for replication. In this case, the performer is truly and hopelessly lost, knowing only that they are in an experiment and are expected to strike the drum periodically at long intervals. This last state of affairs describes the performance at 15 bpm, beat separations of 4 s, which, while showing some diffusion, is also substantially whitened by large point to point fluctuations.

The practical problem of measuring proximity constraints in free rhythmic performance comes down to the detection of random walking or other forms of erratic performance. In the context of synchronized performance (drumming or tapping with a click track), diffusion is not possible, and other statistics must be invented. Below, we review how proximity constraints for the experience of rhythm pulse have been measured in both paradigms as preface to the methods we have adopted here. Recognizing that rhythmic expression is universal in human cultures, it makes sense to begin with a brief discussion of what cultural knowledge tells us about proximity constraints. This is one area of cognitive psychology where some degree of definite knowledge is commonly available.

Prepsychophysics: Cultural Knowledge About Musical Performance

Unlike many of the abilities that are assessed formally using psychophysical techniques, people have been striking drums and playing music for millennia, and consequently, quite a bit is understood about what constitutes appropriate tempi for playing music. We are also in possession of a specific numerical value that is the accepted norm for the slowest tempo that is advised for attempting rhythmical performance. This value is found on metronomes that are fabricated, where the limit is literally set in the materials out of which the metronome is constructed, Seth Thomas metronomes being a prime example. The limiting tempo is 40 bpm, or an interval between beats of 1.5 s. The deliberate instantiation of 40 bpm in hardware reflects tacit knowledge of the psychophysical fact that music played any slower will be quite challenging for performers as well as for conductors who are attempting to signal the quarter note. This limit does not imply that nobody can feel rhythmic pulse at slower tempi, but it does invite caution. The time series shown in Figure A1, although displaying the capacities of a single person, is unequivocally in agreement with the notion that people are rhythmically challenged at tempi slower than 40 bpm.

As a matter of practice, musicians often partition the quarter note interval at slow tempi by counting off subdivisions, something that can be accomplished subvocally. In fact, there is psychophysical evidence that subdividing through counting is a viable and improving strategy for any tempo slower than 50 bpm (Grondin et al., 1999). The obviousness and universality of this strategy suggests that isolated studies reporting that people can competently keep rhythm at tempi slower than 40 bpm (see White, 2017 for some instances) should be questioned. Seth Thomas metronomes represent verified cultural knowledge and unquestionably supply a benchmark for a proximity constraint in rhythmic pulse.

Subjective Assessment of *t-horizon*: Self-Reports of Rhythmic Pulse Disintegration

Comprehensive developmental studies of the human capacity for rhythm have been conducted by Drake et al. (2000) and by McAuley et al. (2006). Both sets of studies develop the entrainment perspective on what makes rhythm possible, and both included a treatment where participants were instructed to tap as slowly as possible while maintaining a "regular" or "smooth" rhythm. To the extent that people are able to competently assess the stability of their tapping performances and so obey these instructions, the tempi they settled on might reflect a measurement of *t-horizon,* effectively the slowest tempo that a person can in fact execute a regular rhythm. However, the results from these studies are in substantial disagreement with each other, with metronome limits, and with other measurements of *t-horizon* that will be reported below.

The slowest attempted performances received by Drake et al. (2000) were statistically characterized in terms of the interbeat interval (or IOI—interonset interval). In their Figure 6, they show a positive monotonic age-related trend with average IOI. As this study was focused mostly on development through childhood, adults in this study are represented as a single point at an IOI of 2 s—adulthood presumably being a single asymptotic state. An IOI of 2 s corresponds to a tempo of 30 bpm, well beyond the limit imposed by manufactured metronomes. This violation does not imply that the adults in this study could not execute regular and smooth performances at 30 bpm, but it does create concern. A tempo of 30 bpm is quite slow (the performance shown in Figure A1 is certainly not stable at 30 bpm), and this suggests that what people might attempt is not commensurate with what they are actually able to achieve in the way of stable rhythmic performance. That there may be a distinction between what people think they can do in slow performance and what they can in fact manage gains additional support from McAuley et al. (2006) who replicated this condition of Drake et al. In Table 2 of McAuley et al., the average IOIs of the slowest attempted performances are listed by age group. McCauley et al. report substantially slower attempted performances than Drake et al.; people in the age range of 8–74 generally attempted slow but regular performances at tempi slower than 24 bpm (2,500 ms IOI). The 10–12-year-old children are especially remarkable in attempting performances near 20 bpm. The fact that identical instructions lead to inconsistent findings, and that the instruction method itself seems to lead to inflated values of the slowest tempi at which rhythmic performance is possible, suggests that the method does not accurately assess *t-horizon*. The problem with both of these studies is that, while they do meaningfully assess what people will attempt, average IOI does not speak to whether the

(*Appendix continues*)

received performances were in fact regular and smooth, that is, whether the performances reflect the instructions.

Time series analyses of drumming performances, described below, are consistent in their finding that people generally cannot produce regular and stable performances below 40 bpm, testimony to the notion that metronome manufacturers in the last century had a good sense of what people are capable of executing. The findings reported in these two studies suggest that either the performances were erratic, and this was not detected, or that the participants subdivided the intertap intervals, and this strategy was not detected. To the first issue, it is not possible to interpret average IOI values deriving from the instruction to tap in a regular and smooth fashion without a subsidiary analysis of the stability of the performances received. An average IOI may be computed on any time series of interbeat intervals, regardless of whether the time series is statistically stationary or whether it displays erratic wandering. The average IOI is, however, only meaningful, having a true convergent value, when computed on a statistically stationary signal. Regarding counting and its detection, if these very slow performances were made possible by subdividing the moments between recorded taps, it is not clear why participants chose to tap every few seconds and not at intervals of tens of seconds or minutes. There is effectively no slowest tempo if subdivision is occurring, and the received data may in this case reflect demand characteristics.

Measurement of *t-horizon* Using Click-Tap Asynchrony in Synchronized Tapping

Mates et al. (1994) appears to have priority in attempting to psychophysically capture the transition tempo that marks the boundary between the experience of rhythmic pulse and the experience of being lost. The logic underlying their method derives from an established but nevertheless curious phenomenon that arises in synchronized tapping (tapping along with a click track) at tempi that are typical of musical performance. When tapping along with an auditory click track, people generally tap ahead of the auditory click track by a few tens of milliseconds. This phenomenon has been investigated in its own right (Aschersleben, 2002) and seems to exist only when the pacing signal and motor tap are separated into two modalities (Müller et al., 2008). Mates et al. interpret negative asynchrony as evidence that people are assembling temporally distributed beats (taps) into templates, and it is the existence of these assemblies that provides the necessary context for beat anticipation. The idea being that only when the beat is anticipatable can the circumstance arise that motor execution reliably leads the auditory feedback. Conversely, at tempi where people cannot feel rhythmic pulse, people lose both the sense of beat groupings into metrical templates, as well as the corresponding ability to anticipate. When beat anticipation fails, the performer must wait for the guiding click track to tell them where in time the beat belongs, and this leads to positive asynchrony. In this way, the transition from negative to positive asynchronies may be used as an implicit signature to infer the integration span for rhythmic pulse.

The utility of this method for inferring proximity constraints on rhythmic pulse depends entirely on the interpretability of the asynchrony distributions. Mates et al. (1994) illustrate the relevant distributions across a range of interbeat intervals (their Figure 2), and the problems with the method are manifest. Similar asynchrony distributions are reported in Matsuda et al. (2015; their Figure 3) and Engström et al. (1996; their Figure 8). Referring to Mates et al., at ISIs of 900 ms and shorter (tempi 67 bpm and faster), the asynchrony distributions are strongly peaked at negative values, recapitulating the basic finding that motivates the method. In addition, the distributions are strongly peaked at positive values at an ISI of 4,800 ms (12.5 bpm), justifying the supposition that there are slow tempi where people are so lost that they must wait for the auditory click track. At these two limits, the situation regarding the feeling of rhythm is clear but hardly an improvement on what is commonly known from musical practice. At intermediate ISIs, the situation regarding template formation is markedly less clear, as the asynchrony distributions straddle zero with increasing variability as a function of ISI in the range [1,200 ms, 3,600 ms]. For the two participants tested in Mates et al., their asynchrony distributions appear to become centered around 0 (neither leading or lagging) at ISI between 1,200 and 1,800 ms. Although not conclusive, centering does get at the notion of being at a transition ISI and suggests that these participants have a *t-horizon* somewhere in this interval. This estimate is consistent both with the idea that counting strategies are recommended when beats are separated by more than 1.2 s (Grondin et al., 1999) and with typical metronome cutoffs at 40 bpm.

Measurement of *t-horizon* Using Time Series Analysis of Tempo Diffusion

Madison (2001) made considerable progress toward the measurement of *t-horizon* through the construction of an algorithm that is sensitive to whether the time series of interbeat intervals is stationary or diffusing as in a random walk. The algorithm has two stages. In the first stage, a diffusion function is computed in terms of how far the interbeat intervals have diverged over the course of w taps, or drum strikes:

$$\Delta(w) = \text{median}\{\text{for all } i : |X(i) - X(i + w)|\}.$$

Here, $X(i)$ is the interbeat interval (essentially the instantaneous tempo) formed between the ith and $(i - 1)$st taps. $\Delta(w)$ is a measure of the typical (in the sense of median) tempo separation over the course of w taps or drum strikes. $\Delta(w)$ will be an increasing function of w if there is growing tempo variation over the course of the performance, and it will fluctuate about zero if the performance stably fluctuates about a single tempo—as is the goal in most musical performances. The derivative of $\Delta(w)$ with w, denoted here by Δ'(tempo), provides a measure of drift rate in the time series of interbeat intervals at a given target tempo. Madison (2001) computes the derivative Δ'(tempo) through the expedient of deriving the slope of $\Delta(w)$ as a function of w in a simple regression model.

Madison (2001, Figure 5) demonstrated that Δ'(tempo) provides a potentially useful statistic for assessing *t-horizon* in the continuation method, at least when aggregated over participants. Most striking is that Δ'(tempo) is relatively small for all performances at target interbeat intervals of 1,300 ms or less and relatively large (by a factor of 2) for all performances at interbeat intervals of 1,400 ms or larger. The existence of a sudden and clear jump in Δ'(tempo) is really quite extraordinary and is the clearest possible signature that rhythm, on average, is compromised at interbeat intervals of 1,400 ms. This value is obviously in substantial agreement with the 1,500 ms built into manufactured metronomes, with the estimate of 1,200–1,800 ms that we deduced from asynchrony distributions of Mates et al., and again, it suggests that the slowest

(*Appendix continues*)

attempted performances recorded by Drake et al. and McAuley et al. may not have been smooth and regular.

Although the diffusion analysis employed by Madison (2001) appears to measure *t-horizon* with much greater resolution than the method based on asynchrony distributions, there are several issues that arise here of a signal detection nature. First, although a nonzero value of Δ'(tempo) might be evidence of the kind of random walking in interbeat interval that indicates that the performer has lost rhythmic pulse (as the 30 bpm performance in Figure A1 depicts), Δ'(tempo) will also take on nonzero values if the performer secularly speeds up or slows down from the target tempo. It is not uncommon for experienced musicians to do this even when they have an intact sense of rhythm. More problematic is that Δ'(tempo) may be close to zero both when the performer is executing a stable performance and also when they are completely lost and executing a white noise of interbeat intervals. Random independent increments will lead to $\Delta(w)$ fluctuating about zero for all values of w, and therefore, so too will be the slope (derivative) of $\Delta(w)$ with w, Δ'(tempo). In view of this dual pathway to zero, Δ'(tempo) may not be monotonically increasing with decreasing tempo. Although Madison's presentation of participant-averaged performances gives the impression that Δ'(tempo) saturates at large values at slow tempi, the analysis of single-participant data from our study will present a more nuanced picture. It will be evident that assessments of *t-horizon* based on this algorithm are not rote.

Measurement of *t-horizon* Using Linear and Nonlinear Methods of Prediction

Gilden and Marusich (2009) developed a number of statistical techniques for assessing *t-horizon* as part of a drumming study designed to characterize the nature of attention deficit hyperactivity disorder (ADHD) temporality. Of note, three of the four statistics characterized the predictability of interbeat intervals. The rationale for focusing on prediction follows from the phenomenology of drumming performance; stable drumming generates fluctuations about a target tempo, while unstable drumming tends to be diffusing. Stable drumming is weakly predictable, in that it expresses a $1/f$ noise (Gilden et al., 1995), while diffusion processes generate hills and valleys in time series portraits. Hills and valleys essentially define what it means to be highly predictable in the context of a stochastic process. The statistics employed were the cv, the lag-1 correlation and its generalization to the power spectrum, and the sample entropy. The cv is not itself a predictive statistic, but in the context of drumming performances, low precision and high predictability tend to co-occur. The power spectrum is aligned with Madison's diffusion rate measure in that the steepness of the power spectrum will covary with the diffusion rate. The sample entropy is a nonlinear measure of predictability that has found application in diagnosis of cardiomyopathy (Richman & Moorman, 2000—predictability of heart beat intervals due to random walking is a signature of disease). All four statistics proved to be useful, and they all converged on a common interpretation.

Nonalgorithmic Measurement of *t-horizon*

The formal approaches that have been developed to measure proximity constraints for rhythmic pulse have the problems encountered generally in methods of signal detection with low resolving power. Distributions of click/tap offsets (Mates et al., 1994; Engström et al., 1996) turn out to have poor resolving power at the level of the individual in the critical tempo regime near 40 bpm where rhythm is compromised. Madison (2001) diffusion rate statistic may be able to resolve the onset of random walking in ensemble averages, but our experience with this statistic, described in the first experiment, is that Δ'(tempo) is not monotonic at the level of the individual. And finally, the predictive statistics employed by Gilden and Marusich (2009) are also inherently noisy, and experience with these statistics have proven that they are ill suited for resolving proximity constraints at the level of the individual. This latter suite of statistics sufficed in the analysis of ADHD temporality only because their coarse resolution could be sharpened through the expedient of ensemble averaging. However, in ordeto investigate allometric laws, each individual must contribute their own unique proximity constraint. At this time, it appears that the inference of individual proximity constraints from rhythmic performance does not have a demonstrable algorithmic solution, and we have been compelled to develop strategies that go beyond formal mathematical characterizations of time series data.

In contexts outside of the analysis of psychological data, there is often recourse to visual inspection. From a formal point of view, what something looks like is mostly controlled by the phase spectrum, aspects of image structure that arise from conditional probabilities connecting three or more points. The statistics employed by Gilden and Marusich (2009) and Madison (2001) are mostly picking up information that is contained in the power spectrum, image information arising from conditional probabilities connecting two points. This distinction, although somewhat technical, is critical to image analysis. If the visual system used only the statistics that have been used to algorithmically assess *t-horizon,* we would be essentially blind, unable to recognize objects, and living in a world consisting only of oriented light and dark patches. It is a fact that most of the information in drumming time series is not being picked up by the statistics that have been used, and this is a handicap that is not necessary.

Visual assessments of data are not typically a part of confirmatory statistical analysis, bias being an obvious problem, but in the context of allometry, bias may be substantially mitigated through ignorance. Visual inspection of drumming time series with the purpose of finding the inflection tempo where the performer loses rhythmic pulse would be permissible so long as the assessment is done in ignorance of the performer's body size. In this way, the visual inspection would not be able to create an allometry beyond whatever chance could supply. A second problem with visual analysis is that it is not rote because it is not explicitly algorithmic. In the same way that an experienced physician can read a magnetic resonance image better than a novice, a person who has been looking at drumming data for some time may see things that a novice might not. Considerations of expertise are not welcome in statistical analysis, but it is a problem here only in the sense that, if the people judging our time series are not familiar with the domain of interbeat intervals, the worse they can do is generate noise in whatever underlying allometric relations may exist. The technique of visual analysis to locate *t-horizon* is described and illustrated in the main text.

Received August 2, 2019
Revision received March 17, 2021
Accepted May 9, 2021 ■